

piggyBac transposons expressing full-length human dystrophin enable genetic correction of dystrophic mesoangioblasts

Mariana Loperfido^{1,2}, Susan Jarmin³, Sumitava Dastidar¹, Mario Di Matteo^{1,2}, Ilaria Perini⁴, Marc Moore³, Nisha Nair¹, Ermira Samara-Kuko¹, Takis Athanasopoulos^{3,5}, Francesco Saverio Tedesco⁶, George Dickson^{3,†}, Maurilio Sampaolesi^{4,†}, Thierry VandenDriessche^{1,2,†} and Marinee K. Chuah^{1,2,*,†}

¹Department of Gene Therapy & Regenerative Medicine, Free University of Brussels, Brussels 1090, Belgium, ²Center for Molecular & Vascular Biology, Department of Cardiovascular Sciences, University of Leuven, Leuven 3000, Belgium, ³School of Biological Sciences, Royal Holloway, University of London, Egham, Surrey, TW20 0EX, UK, ⁴Translational Cardiomyology Laboratory, Embryo and Stem Cell Biology Unit, Department of Development and Regeneration, University of Leuven, Leuven 3000, Belgium, ⁵Faculty of Science & Engineering, University of Wolverhampton, Wolverhampton, WV1 1LY, UK and ⁶Department of Cell and Developmental Biology, University College London, London, WC1E 6DE, UK

Received August 13, 2015; Revised November 25, 2015; Accepted November 28, 2015

ABSTRACT

Duchenne muscular dystrophy (DMD) is a genetic neuromuscular disorder caused by the absence of dystrophin. We developed a novel gene therapy approach based on the use of the *piggyBac* (*PB*) transposon system to deliver the coding DNA sequence (*CDS*) of either full-length human dystrophin (*DYS*: 11.1 kb) or truncated microdystrophins (*MD1*: 3.6 kb; *MD2*: 4 kb). *PB* transposons encoding microdystrophins were transfected in C2C12 myoblasts, yielding 65±2% MD1 and 66±2% MD2 expression in differentiated multinucleated myotubes. A hyperactive *PB* (*hyPB*) transposase was then deployed to enable transposition of the large-size *PB* transposon (17 kb) encoding the full-length *DYS* and green fluorescence protein (GFP). Stable GFP expression attaining 78±3% could be achieved in the C2C12 myoblasts that had undergone transposition. Western blot analysis demonstrated expression of the full-length human *DYS* protein in myotubes. Subsequently, dystrophic mesoangioblasts from a Golden Retriever muscular dystrophy dog were transfected with the large-size *PB* transposon resulting in 50±5% GFP-expressing cells after stable transposition. This was consistent with correction of the differentiated dystrophic mesoangioblasts following expression of

full-length human *DYS*. These results pave the way toward a novel non-viral gene therapy approach for DMD using *PB* transposons underscoring their potential to deliver large therapeutic genes.

INTRODUCTION

Duchenne muscular dystrophy (DMD) is amongst the most severe forms of muscular dystrophies, affecting up to 1 in 5000 boys (1). DMD is an X-linked disorder caused by mutations or deletions in the gene encoding dystrophin (2), which is required for the assembly of the dystrophin-glycoprotein complex (3,4). This complex is responsible of maintaining the integrity of the sarcolemma during muscle contraction, providing a mechanical and functional link between the cytoskeleton of the muscle fiber and the extracellular matrix. The absence of dystrophin causes DMD, a severe inheritable myopathy with its onset in the first years of life. This pathology leads to a progressive muscle weakness, consistent with fiber degeneration, inflammation, necrosis and replacement of muscle with scar and fat tissue (5). Impairment of the patient's daily functional abilities rapidly results in a profound reduction in quality of life together with a shortened life expectancy, mainly due to cardiac and respiratory failure. The current standard of care involves the use of anti-inflammatory and immunosuppressive drugs (e.g. corticosteroids), that have shown to modestly improve muscle function (6–9), prolonging the patient's life expectancy up to 30 years of age. Nevertheless, it is necessary to develop

*To whom correspondence should be addressed. Tel: +32 477529653; Fax: +32 24774159; Email: marinee.chuah@vub.ac.be

†These authors share joint senior authorship.

effective therapies that also counteract muscle degeneration in DMD patients and have a more profound impact of the patient's quality of life and life expectancy.

Several approaches are currently being pursued to address this unmet medical need, aimed at restoring dystrophin expression (10,11). Exon-skipping approaches based on antisense oligonucleotides had been proposed as a promising strategy to correct the reading frame and restore dystrophin expression (12,13). However, exon skipping is only applicable to a subset of patients with specific mutations and ultimately leads to the production of a truncated dystrophin protein, similar to that found in patients affected by Becker muscular dystrophy (BMD). This is a milder allelic form of muscular dystrophy, that can still cause significant disability (14,15). Consequently, exon-skipping does not replicate and fully reconstitute all of the essential functions of dystrophin (16,17). Although encouraging, exon skipping therapies are only recently entering clinical experimentation in larger patient cohorts, with unclear efficacy results in some cases (18).

Gene therapy for DMD is particularly challenging given the large size of the dystrophin gene (2.4 Mb) and its corresponding *CDS* (11.1 kb) (19,20). Moreover, *in vivo* gene therapy using viral vectors like helper-dependent adenoviral vectors are able to provide the full-length dystrophin *CDS*, but show limitations related to the delivery of a therapeutic dose to the entire body musculature (21,22). Adeno-associated viral (AAV) vectors might be considered as a good alternative for an efficient systemic delivery in the muscles, but their use is impeded by their restricted packaging capacity (23–26). This precludes gene therapy with the full-length human dystrophin *CDS* and requires truncated human dystrophin isoforms instead. Moreover, the use of viral vectors may evoke potential immune responses against the vector and/or the gene-modified cells (27–30). Hence, there is a need to develop strategies that allow for efficient and safe delivery of the full-length dystrophin *CDS*.

In the current study, we therefore validated a new gene therapy approach that aims to overcome some of these limitations, allowing stable gene delivery of the full-length human dystrophin *CDS*. To achieve this goal, we explored the use of a hyperactive *piggyBac* (*PB*) transposon system, that reportedly can accommodate relatively large inserts (31–33). *PB* transposons, originally identified in the cabbage looper moth *Trichoplusia ni* (34,35), have been adapted for use in mammalian cells, following codon-usage optimization and incorporation of several hyper-activating mutations (33,36–38). For gene therapy, an expression plasmid that encodes for the *PB* transposase is transiently transfected along with a donor plasmid containing the therapeutic gene, flanked by the transposon terminal repeat sequences (39). The binding of the *PB* transposase in the terminal repeat sequences enables transposition via a cut-and-paste mechanism (40). To develop a *PB* transposon-based stem cell/gene therapy approach for DMD, we chose to employ mesoangioblasts (MABs) (41–43). MABs are mesodermal vessel-associated stem/progenitor cells that have the capacity to cross the vessel wall upon intra-arterial transplantation and contribute to the regeneration of dystrophic muscles (44–48). This occurs either by direct fusion with the muscle or by entering the muscle satellite cell niche

(43,47). The therapeutic potential of MABs has been investigated in a recently completed phase I/II clinical trial based on the intra-arterial transplantation of allogeneic cells in five DMD patients under immunosuppressive regimen (EudraCT N° 2011–000176–33) (49). The outcome of this study provides new insights primarily on the safety and partially on the efficacy of the use of MABs to treat DMD patients. Moreover, this approach differed from other clinical trials based on the intravenous administration of cells that get trapped in the filter organs (50,51). Thus it represents the starting point for the development of efficient cell therapy protocols for DMD based on the use of gene-modified autologous MABs with the advantage over allogeneic MABs to possibly avoid the immune suppression.

Therefore, in the current study, we provided - for the first time - proof of concept that the hyperactive *PB* transposons are well suited to genetically correct dystrophic MABs, by delivering the full-length human dystrophin *CDS*.

MATERIALS AND METHODS

Cell cultures

C2C12 myoblasts (91031101; Sigma-Aldrich; (52)) were cultured, as previously described (53), in D20 medium composed of high glucose Dulbecco's modified Eagle's medium (DMEM; Life Technologies) supplemented with 20% Fetal Bovine Serum (FBS; Life Technologies), 2 mM L-glutamine (Life Technologies), 100 IU/ml penicillin and 100 µg/ml streptomycin (P/S; Life Technologies), at 37°C in a 5% CO₂ cell culture incubator. A biopsy from a Golden Retriever muscular dystrophy (GRMD) dog was kindly provided by Dr Richard from Le Centre de Boisbonne-ONIRIS (Nantes-Atlantique, France). Canine mesoangioblasts (MABs) were isolated and maintained in culture, as described previously (45,53). Briefly, a biopsy from the *vastus lateralis* muscle of a 10-month-old male dog was minced in 1mm² pieces. These fragments were transferred onto collagen type I-coated dishes (Sigma-Aldrich) and incubated in growth medium composed of MegaCell DMEM (Sigma-Aldrich) containing 5% FBS (Life Technologies), 0.1 mM β-mercaptoethanol (Life Technologies), 1% MEM non-essential amino acids (Life Technologies), 1% P/S, 1% L-glutamine, 5 ng/ml human basic fibroblast growth factor (Peprotech) at 37°C in a 5% CO₂, 3% O₂ cell culture incubator. After 5 to 7 days, small, round, refractile cells (Supplementary Figure S1A) that adhered weakly to the initial cell outgrowth were identified. This cell population was collected and maintained in growth medium on collagen-coated flasks. In order to confirm that the identified population was composed of *bona fide* MABs, cells were characterized for the typical markers of adult dog MABs, after five and ten passages (Supplementary Figure S1B–E). The alkaline phosphatase expression was detected by enzymatic activity using the NBT/BCIP kit (Roche). The staining was performed on fixed cells in order to allow the formation of a black/purple precipitate in the cells expressing the enzyme (Supplementary Figure S1B). Moreover, their capacity to differentiate into mesodermal lineages was analyzed by assessing their intrinsic differentiation potential into multinucleated skeletal myotubes or, under appropriated stimuli, into smooth muscle cells (Supplementary Figure S1F, SG;

see specific section 'In vitro differentiation assay'). Human skeletal muscle cells (SKM; C-12530; Promocell) were used as positive control and cultured in the same condition of GRMD MABs.

Transposase and transposon constructs

The *piggyBac* (*PB*) transposase constructs encoding the native *PB* transposase (*mPB*) or the hyperactive *PB* transposase (*hyPB*) were described previously (54). An identical expression plasmid devoid of the *PB* transposase gene (denoted as empty) was used as control (Figure 1). The *PB* transposon constructs were generated after synthesis of the wild type sequences of the *PB* terminal inverted repeats (*IRs*; Gene Synthesis, Canada) and cloning into the *pBluescript II SK (+)* plasmid upon digestion with *BssHIII* restriction enzyme (55,56). To produce the transposons *PB-SPc-MD1* and *PB-SPc-MD2*, the muscle-specific synthetic promoter *SPc5-12* (57) was amplified with primers (forward: 5'-ATAGCTAGCCAGATCGAGCTCCACCGCGGT-3'; reverse: 5'-ATAACGCGTGAATTCCTGCAGCCCGGG-3') adding flanking *NheI* and *MluI* restriction sites, and ligated between the 5' and 3' *IRs*. This intermediate plasmid, designated as *PB-SPc5-12*, was used to insert the codon-usage optimized *CDS* of human microdystrophin *MD1* or *MD2* (58,59), together with the simian virus 40 (SV40) late polyadenylation (pA) signal, after amplification with primers (forward: 5'-ATAACGCGTGCCACCATTGCTGTGGTGGGAG-3'; reverse: 5'-ATACTCGAGGTTTATTGCAGCTTATAATGGTTACAAATAAAGCAATAGCATCA-3') and digestion with *MluI* and *XhoI* restriction enzymes. To generate the transposon *PB-SPc-GFP*, the SV40 pA sequence was amplified with primers (forward: 5'-ATAACGCGTCAGACATGATAAGATACATTGATG-3'; reverse: 5'-ATACTCGAGGTTTATTGCAGCTTATAATGGTT-3') adding flanking *MluI* and *XhoI* restriction sites, and ligated into the intermediate plasmid *PB-SPc5-12*. Then the transgene copepod GFP (Lonza) was PCR-amplified (forward: 5'-ATAACTAGTAGCGCTACCGGTCGCCACC-3'; reverse: 5'-ATAACGCGTAGATCTGGCGAAGGCATGGG-3') flanked by *SpeI* and *MluI* restriction sites and cloned between the *SPc5-12* promoter and the SV40 pA signal. To produce the transposon *PB-Pgk-GFP*, the PCR primers (forward: 5'-GTACGGCTAGCGTTAACAATTCTACCGGGTAGG-3', reverse: 5'-GACGTAGCGCTATGCAGGTCGAAAGGC-3') containing *NheI* and *Eco47III* restriction sites were used to amplify the *Pgk* promoter (Addgene) and cloned it into the correspondent sites of *PB-SPc5-12* in order to replace *SPc5-12* promoter. For the construction of the large size transposon *PB-SPc-DYS-Pgk-GFP*, the following fragment *SPc5-12 promoter-KpnI-NheI-SgsI-SV40 pA signal* has been synthesized (DNA cloning, Germany) adding flanking restriction sites *NotI* and *XhoI*, and inserted between the 5' and 3' *PB IRs* of the *pBluescript II SK (+)* plasmid. This allowed the ligation of the codon usage optimized full-length human dystrophin *CDS* (Jarmin *et al.*, unpublished) upon digestion first with *KpnI* and *NheI*, and then with *NheI* and *SgsI* restriction enzymes.

The GFP reporter gene was then inserted together with the *Pgk* promoter and the SV40 pA signal downstream the full-length human dystrophin expression cassette using *HpaI* and *XhoI* restriction sites. The entire expression cassette of all the *PB* transposons was flanked with *loxP* sites allowing for a possible subsequent excision by CRE recombinase (39,60). The sequences of the constructs involving PCR-based cloning were confirmed by DNA sequencing.

Transfection

Cells were electroporated with the Amaxa Nucleofector II (Lonza). For C2C12 myoblasts, the Cell Line Nucleofector Kit V and the program B-32 were used. Whilst for GRMD MABs, the Human MSC Nucleofector Kit and the program U-23 were applied. Transfections were optimized to obtain good efficiency with low levels of toxicity, modifying the amount of plasmids used and the transposase: transposon ratio. Briefly, cells were trypsinized, washed in PBS (Life Technologies) and counted; 1×10^6 cells were electroporated and subsequently seeded in a single dish of a 6-well multidish (Nunc). The day after, the medium was replaced with fresh medium. Transfection efficiency was assessed by calculating the percentage of GFP+ cells at 24, 48 and 72 h post-electroporation (EP) by fluorescence microscopy and/or fluorescence activated cells sorter (FACSCanto™ flow cytometer, Becton Dickinson). In this case, transfected C2C12 cells or GRMD MABs were therefore trypsinized, washed in PBS, counted and resuspended into PBS supplemented with 1% FBS and 2mM EDTA (Life Technologies). Analyses were performed with FACSDiva software. Where indicated, GFP positive C2C12 cells or GRMD MABs were enriched respectively at day 4 and 7 days post-EP by FACS sorting (BD FACSAria, Becton Dickinson). Transfected cells were monitored for 28–30 days post-EP to assess transposition efficiency.

Transduction

GRMD MABs were transduced with a lentiviral vector containing a tamoxifen-inducible MyoD-ER expression cassette (61) to induce myogenic differentiation at late passages (i.e. passage P15–18). Lentiviral vector titration was calculated based upon the p24 assay (QuickTiter Lentivirus Quantitation Kit, Cellbiolabs). Working concentrations were determined by assessing myogenic differentiation efficiency at increasing multiplicities of infection (MOI). Briefly, 0.14×10^6 cells were transduced with 1, 5 or 50 MOI of MyoD-ER lentiviral vector in 1 ml of culture medium and incubated for 12 h at 37°C in a 5% CO₂, 3% O₂ cell culture incubator. Media were subsequently changed and cells maintained in culture for 2–3 passages, after which the *in vitro* differentiation assay into skeletal muscle was performed (see specific section below). The optimal condition was set at 50 MOI.

In vitro differentiation assays

The ability of C2C12 cells, GRMD MABs and SKM cells to differentiate into skeletal muscle was assessed *in vitro* by

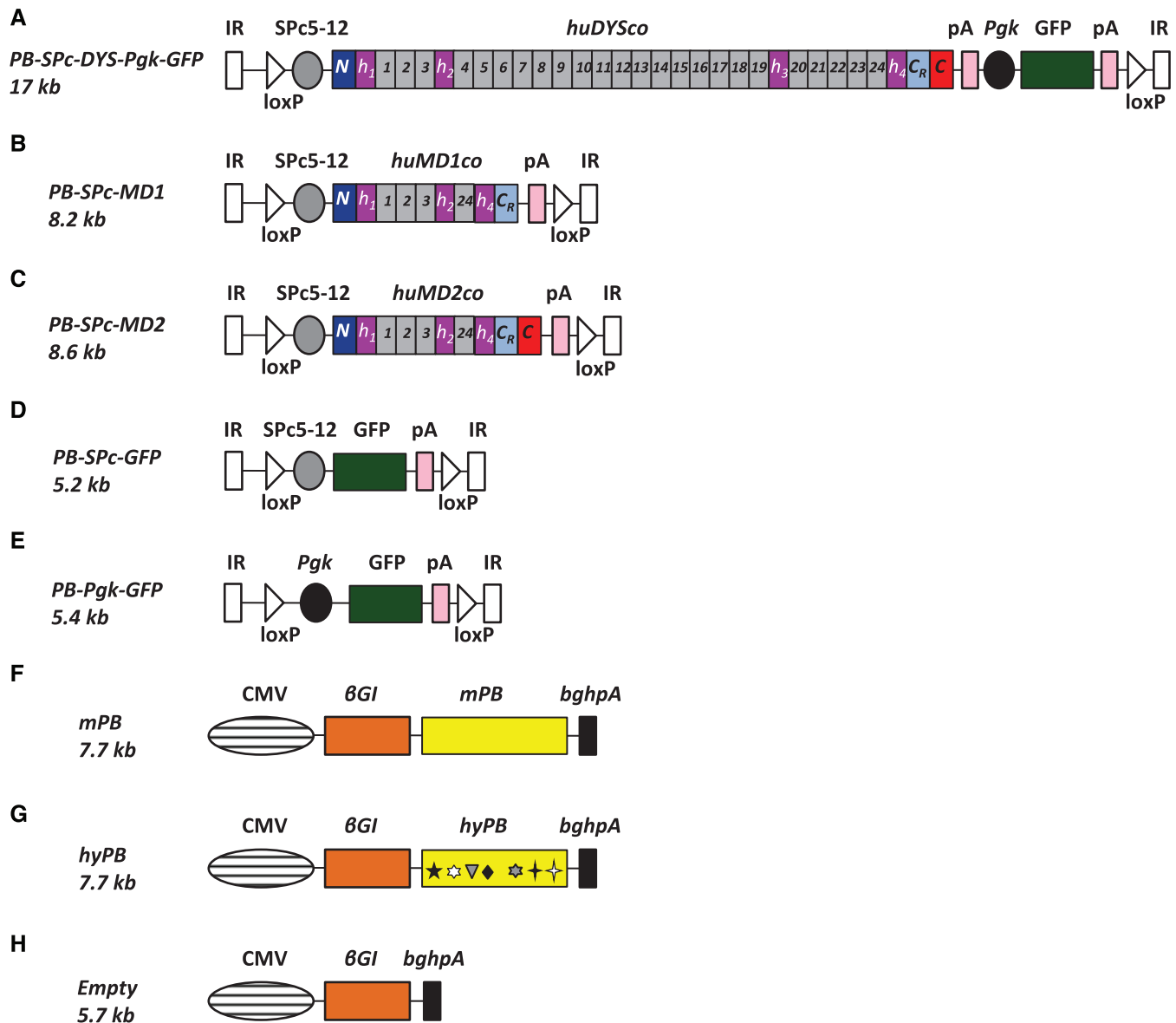


Figure 1. Schematic representation of *PB* transposon and *PB* transposase constructs. (A) *PB-SPc-DYS-Pgk-GFP* transposon encoding the codon optimized full-length human dystrophin *CDS* (*huDYSco*; (59)) is represented as in its four major structural domains: N-terminal domain (N), a central rod domain, a cysteine-rich (CR) domain and a distal C-terminal domain (C). The central rod domain contains 24 triple-helix rod repeats and four hinges (H1–H4). The full-length human dystrophin *CDS* is driven by the muscle-specific synthetic promoter SPC5–12 (57). Downstream, the sequence of a copepod GFP has been cloned as a reporter driven by the *Pgk* promoter. (B,C) *PB-SPc-MD1* and *PB-SPc-MD2* transposons encode respectively for *huMD1co* and *huMD2co* *CDS*; these are two different codon optimized human microdystrophins that lack the original sequence of rod repeats 4–23 and differ for the presence of the C-terminal domain sequence in *MD2* (59). This extra sequence has been shown to improve the efficiency on restoring muscle function in dystrophic *mdx* mice (58). Both the microdystrophins are driven by SPC5–12 promoter. (D,E) *PB-SPc-GFP* and *PB-Pgk-GFP* are transposons that accommodate the GFP sequence respectively under the SPC5–12 or the *Pgk* promoter. All the transposon constructs are flanked by wild-type inverted repeats (IR) and loxP sites (loxP). All the transgenes in the transposon constructs are followed by the simian virus 40 late polyadenylation signal (pA). The transposase constructs are instead represented from (F) to (H) (54).

exposing the cells upon reaching 80% of confluence to a specific differentiation medium composed of DMEM supplemented with 2% horse serum (Euroclone), 1% P/S, 1% L-glutamine for 4 to 10 days (53). C2C12 cells were induced to differentiate on a 6-well multidish (Nunc), while GRMD MABs and SKM cells were seeded onto matrigel (BD Biosciences) coated dishes. When cells were transduced with the tamoxifen-inducible MyoD-ER lentiviral vector, 1 μ M 4-hydroxy-tamoxifen (Sigma-Aldrich) was added in

the growth medium that was replaced 24 h later by differentiation medium supplemented with 1 μ M 4-hydroxy-tamoxifen. Half of the medium was replaced with fresh differentiation medium every other day. Immunofluorescence (IF) staining for myosin heavy chain (MyHC) was performed to confirm multinucleated myotubes (see specific section for 'IF staining'). Differentiation of GRMD MABs in smooth muscle-like cells was induced by treating the cells for 10 days with differentiation medium supplemented with

5 ng/ml transforming growth factor β 1 (Sigma-Aldrich) (62). Smooth muscle differentiation was confirmed by IF staining for α -smooth muscle actin (α SMA; see specific section for 'IF staining').

Flow cytometry

Expression of CD44, CD34 and CD45 markers on GRMD MABs was assessed after incubating the cells with specific anti-dog fluorochrome-conjugated monoclonal antibodies for 1 hour at 4°C: anti-CD44-APC (FAB5449A; R&D Systems), anti-CD34-PE (559369; BD Biosciences), anti-CD45-RPE (MCA1042PE; AbD Serotec). Cells were subsequently washed with PBS and fixed in 2% paraformaldehyde (Sigma-Aldrich). Cytofluorimetric analysis was performed using a FACSCanto™ flow cytometer and FACS-Diva software. At least 10,000 events were acquired for each sample.

Immunofluorescence staining

In vitro differentiated C2C12 cells or GRMD MABs were washed with PBS (Sigma-Aldrich), fixed with 4% paraformaldehyde (Sigma-Aldrich) at room temperature (RT) for 10 min and permeabilized with PBS containing 0.2% Triton X-100 (Sigma-Aldrich) and 1% BSA (Sigma-Aldrich) at RT for 30 min. As a blocking solution, 10% donkey serum (Sigma-Aldrich) was used at RT for 30 min to reduce secondary antibody background signal. The cells were subsequently incubated overnight at 4°C with the following primary antibodies: rabbit anti-turboGFP (AB513; Evrogen), mouse anti-dystrophin (NCL-DYS1, NCL-DYS2, NCL-DYS3; Novocastra), mouse anti-myosin heavy chain (MyHC MF20; Developmental Studies Hybridoma Bank, USA), rabbit anti-myosin (476126; Calbiochem), mouse anti-myogenin (F5D; Developmental Studies Hybridoma Bank, USA), rabbit anti-MyoD (M-318; Santa Cruz), mouse anti-sarcomeric α -actinin (ab9465; Abcam), mouse anti- α smooth muscle actin (A2547; Sigma-Aldrich). After incubation, cells were washed with PBS and then incubated with the appropriate 488, 546, 594 or 647-fluorochrome conjugated secondary antibodies (Life Technologies) together with Hoechst 33342 for nucleic acid staining (B2261; Sigma-Aldrich) for 1 hour at RT in PBS containing 0.2% Triton X-100. After three successive washings with PBS, slides were mounted using fluorescent mounting medium (Dako) and examined by fluorescence microscopy (DMI6000B, Leica, Germany). Images were analyzed using ImageJ software (NIH; <http://rsbweb.nih.gov/ij/download.html>). The monoclonal antibody MF20 developed by Donald Fischman was obtained from the Developmental Studies Hybridoma Bank (DSHB) developed under the auspices of the National Institute of Child Health and Human Development (NICHD) and maintained by the University of Iowa, Department of Biology, Iowa City, IA 52242.

Western blot

To assess the *PB*-mediated expression of the full-length human dystrophin protein, C2C12 cells differentiated into

skeletal muscle *in vitro* were washed with cold PBS and lysed in RIPA buffer in presence of Complete Mini protease inhibitor mixture (Roche) for 30 min on ice. Cell lysates were cleared and quantified. The following non-conjugated primary antibodies were used: mouse anti-human dystrophin (NCL-DYS3; Novocastra) and mouse anti-myosin heavy chain (MyHC MF20; Developmental Studies Hybridoma Bank, USA). As secondary antibody, the HRP-conjugated goat anti-mouse (Santa Cruz) was used. To detect a housekeeping protein, the HRP-conjugated anti-beta-tubulin (Abcam) was used. Signal was visualized by Enhanced Chemiluminescent Reagents (ECL, Invitrogen) or West Femto (Thermo Scientific), according to the manufacturer's instructions. SKM cells differentiated into skeletal muscle *in vitro* were used as positive control.

RNA analysis

Total RNA was extracted (RNeasy Mini Kit, QIAGEN) and reversed transcribed using a cDNA synthesis kit (SuperScript® III First-Strand synthesis system for RT-PCR kit, Life Technologies). For RT-PCR, cDNA was amplified on a PCR thermocycler (Biorad) with GoTaq DNA Polymerase (Promega). Amplifications were performed using the primers listed in Supplementary data, Table S1, at the annealing temperature of 60°C for 25 cycles on C2C12 and 29 cycles on GRMD MABs. The amplified fragments were resolved by electrophoresis on a 2% agarose gel. For quantitative RT-PCR (qRT-PCR), cDNA was amplified on a Step-One Real-Time PCR System (Applied Biosystems; Life technologies) with SYBR green PCR Master mix (Applied Biosystem). In particular, the semi-quantitative RT-PCRs for the characterization of GRMD MABs were performed by using the primers listed in Supplementary data, Table S2, at the annealing temperature of 60°C for 33 cycles. Amplicons were then resolved by electrophoresis on a 2% agarose gel. Whilst the transgene mRNA levels in treated and untreated C2C12 cells and GRMD MABs were determined by qRT-PCR, using the primers described in Supplementary data, Table S3. Data were normalized to the GAPDH housekeeping gene or to the MyHC gene specific for the skeletal muscle differentiation. The expression levels of the selected transgene was calculated using a standard $\Delta\Delta C_t$ method (63).

Transposon copy number

The number of copies of *PB* transposon integrated per cell (diploid genome) was calculated by performing a qPCR on genomic DNA (DNeasy Blood & Tissue Kit, Qiagen) by using primers specific for the 5' inverted repeat region (5' IR) of the *PB* transposon, as previously described (54). The standard curve was determined by a known copy number of the corresponding *PB* transposon plasmid.

Statistical analysis

Data were presented as mean and standard deviation (SD) or standard error of the mean (SEM). Comparison between groups was performed by using two-tailed unpaired Student's t-test or two-way ANOVA (Bonferroni's multiple comparison test).

RESULTS

Generation of *PB* transposons encoding for human dystrophin *CDS*

We generated *PB* transposons designed to express the full-length or truncated versions of a codon-optimized human dystrophin *CDS* (59) from the muscle-specific synthetic promoter SPc5–12 (346 bp) (57,58,64) (Figure 1). The simian virus 40 (SV40) late polyadenylation signal (pA) was incorporated as transcription terminator in all the expression cassettes. Given the large cargo that *PB* transposons could accommodate (32,33), we generated a large-size transposon named *PB-SPc-DYS-Pgk-GFP* encoding for the full-length human dystrophin *CDS* (*huDYSco*; size: 11.1 kb) driven by the synthetic SPc5–12 promoter, and a GFP reporter transgene driven by the constitutive phophoglycerate kinase 1 (*Pgk*) promoter (transposon size: 17 kb) (Figure 1A). *PB-SPc-MD1* (Figure 1B) and *PB-SPc-MD2* (Figure 1C) transposons encoded respectively for two different codon usage-optimized microdystrophin *CDS*: *huMD1co* (size: 3.6 kb) and *huMD2co* (size: 4 kb) whereby the C-terminal domain was deleted in *huMD1co* (58) (transposon size: 8.2 kb and 8.6 kb, respectively). As controls, *PB-SPc-GFP* (Figure 1D) and *PB-Pgk-GFP* (Figure 1E) transposons carried only the copepod GFP sequence under the control of the SPc5–12 or the constitutive *Pgk* promoter (transposon size: 5.2 kb and 5.4 kb, respectively). The transposase plasmids included the *mPB* expression plasmid, encoding the murine codon-optimized, non-hyperactive *PB* transposase (Figure 1F) and the *hyPB* expression plasmid encoding the murine codon-optimized, hyperactive *PB* transposase (Figure 1G). An empty plasmid that contained an identical expression cassette, but devoid of transposase (Figure 1H), was employed as control (54).

Expression of human microdystrophins after *PB*-mediated transposition in C2C12 myoblasts

We first tested the functionality of the *PB-SPc-GFP*, *PB-SPc-MD1* and *PB-SPc-MD2* transposons since they are smaller in size and therefore easier to transfer into the target cells. C2C12 cells, a murine myoblast cell line (52), were co-transfected by electroporation with the *PB-SPc-GFP* transposon and the *mPB* transposase-encoding construct (ratio of 1.26 pmol transposase DNA: 3.48 pmol transposon DNA). In parallel, *PB-SPc-MD1* and *PB-SPc-MD2* transposons were electroporated under the same conditions. To determine the transfection efficiency of *mPB* transposase and *PB-SPc-GFP* transposon, FACS analysis was performed 48 h post-electroporation (EP), showing 26±4% GFP+ cells which remained relatively stable (24 ± 4% GFP+ cells at 72 h post-EP; not statistically significant) (Figure 2A, left panel). As control, the empty expression plasmid- devoid of *mPB* transposase gene- was electroporated with the *PB-SPc-GFP* transposon resulting initially in comparable transfection efficiencies at 48 h (17 ± 1% GFP+ cells). However, in contrast to when the *mPB* expression vector was employed, the percentage of GFP+ transfected cells gradually declined at 72 h post-EP, consistent with the loss of non-integrated *PB-SPc-GFP* plasmids in the rapidly dividing C2C12 cells (9±1% GFP+ cells; $p \leq 0.01$). Simi-

larly, the mean fluorescent intensity (MFI) was sustained when the *PB-SPc-GFP* transposon was co-transfected with *mPB* and significantly different from the controls ($p \leq 0.001$) (Figure 2A, right panel). These FACS data were confirmed by live cell imaging (Figure 2B).

Subsequently, we assessed whether C2C12 cells transposed with the *PB* transposons retained their ability to differentiate into skeletal muscle and whether expression of the GFP and microdystrophins MD1 and MD2, encoded by the transposons, was sustained upon differentiation. Four days after incubation with the differentiation medium (corresponding to 10 days post-EP), multinucleated myotubes were observed. The transcription levels of GFP (Figure 2C) and the human microdystrophins MD1 and MD2 (Figure 2D) were detectable by qRT-PCR and showed a significantly increased expression upon differentiation ($P \leq 0.01$ for GFP, $P \leq 0.001$ for the microdystrophins). This confirmed the muscle-specificity of the synthetic SPc5–12 promoter, consistent with its up-regulation upon myogenic differentiation. The transcript levels of the microdystrophins MD1 and MD2 in the differentiated C2C12 cells were comparable to the level of human dystrophin transcripts in differentiated human skeletal muscle (SKM) cells (Figure 2D). In contrast, we were not able to detect any GFP expression from differentiated C2C12 cells that were co-transfected with the empty plasmid and the *PB-SPc-GFP* transposon (Figure 2C). This indicates that transposition was a prerequisite to ensure stable GFP transcript levels. Immunofluorescence (IF) staining independently confirmed GFP (Figure 2E) and human microdystrophin MD1 and MD2 expression (Figure 2F) respectively in the myosin heavy chain (MyHC) and myosin positive myotubes, derived from the transposed C2C12 cells. The percentage of myotubes positive for GFP, MD1 or MD2 was determined by counting the nuclei within these myotubes divided by the total number of nuclei within the MyHC positive myotubes (68±6% for GFP; 65±2% for MD1 and 66±2% for MD2, respectively). Collectively, these results demonstrate that the *PB* transposon system is well suited to achieve sustained muscle-specific expression of human microdystrophins upon transposition in differentiated myogenic cells. The validation of the *PB* transposon system for the delivery of the truncated human dystrophins paves the way toward the use of the full-length human dystrophin.

Increased transposition in C2C12 myoblasts with the hyperactive *PB* transposase and the *PB* transposon encoding the full-length human dystrophin *CDS*

Different research groups, including ours, have shown that the *hyPB* transposase resulted in increased transposition as compared to the *mPB* transposase (37,38,54,65). In line with these results, we therefore assessed the transposition efficiency of *hyPB* transposase in a head-to-head comparison with the *mPB* transposase, along with the large-size transposon *PB-SPc-DYS-Pgk-GFP* (17 kb) in C2C12 myoblasts. This represents the first attempt in delivering the full-length dystrophin *CDS* by the *PB* transposon system. The *mPB* or *hyPB*-encoding expression constructs were electroporated together with *PB-SPc-DYS-Pgk-GFP* transposon in C2C12 myoblasts (ratio of 0.32 pmol transposase DNA: 0.87 pmol transposon DNA). Controls were transfected with the empty expression plasmid devoid of any

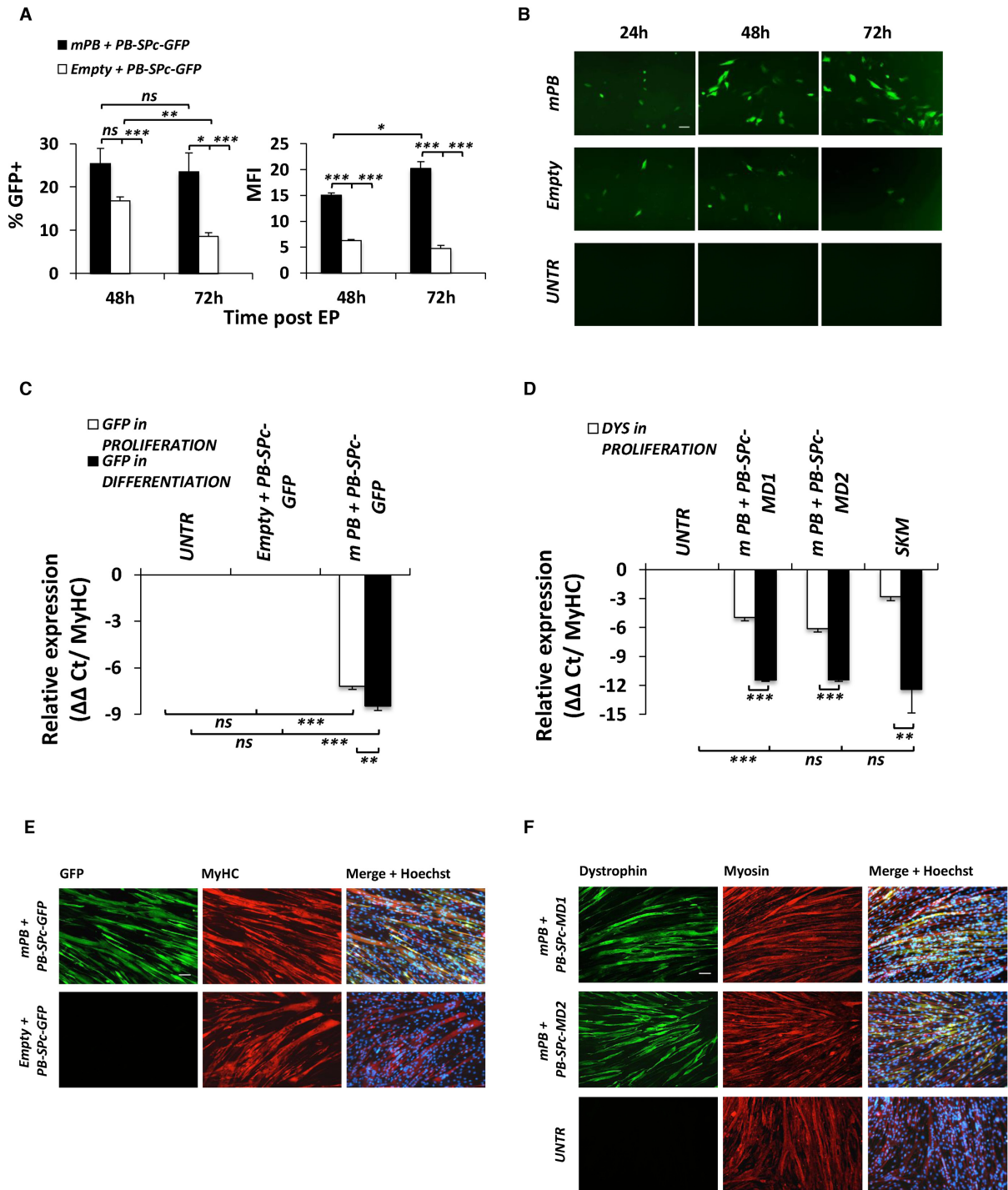


Figure 2. PB-mediated expression of MD1 and MD2 in C2C12 myoblasts. (A) The bar graphs show respectively the percentage of GFP+ (left) and the mean fluorescence intensity (MFI; right) of C2C12 cells at 48 and 72 h post-electroporation (EP) with the PB-SPc-GFP transposon when co-transfected with the native mPB transposase or the empty plasmid (ratio of 1.26 pmol transposase DNA: 3.48 pmol transposon DNA). Untransfected cells are also shown. Shown are mean \pm SEM of three independent biological replicates; two-tailed unpaired Student's t-test ($***P \leq 0.001$; $**P \leq 0.01$; $*P \leq 0.05$; ns: not significant). (B) Live cell imaging showing the GFP expression of the conditions described in (A) at 24, 48 and 72 h post-EP (UNTR: untransfected; scale bar 100 μ m). (C,D) The bar graphs depict the transcript levels of GFP (C) or MD1 and MD2 (D) detected by qRT-PCR in PB-transposed C2C12 myoblasts in proliferation (white bars) and myotubes in differentiation (black bars). The transcript levels of the human dystrophin from the human skeletal muscle (SKM) cells and myotubes were used as positive control. Values were normalized for the myosin heavy chain (MyHC) and shown as relative expression. Shown are mean \pm SEM of triplicate qRT-PCR analyses performed for three independent biological replicates; two-tailed unpaired Student's t-test ($***P \leq 0.001$; $**P \leq 0.01$; ns: not significant). (E,F) Immunofluorescence staining on transposed C2C12 cells upon skeletal muscle differentiation *in vitro* has been used to detect the GFP expression (E, in green) in MyHC positive myotubes (E, in red), or the human microdystrophins MD1 and MD2 expression (F, in green) in myosin positive myotubes (F in red). The nuclei were stained with Hoechst (Scale bar 100 μ m). The mouse anti-human dystrophin NCL-DYS3 antibody was used.

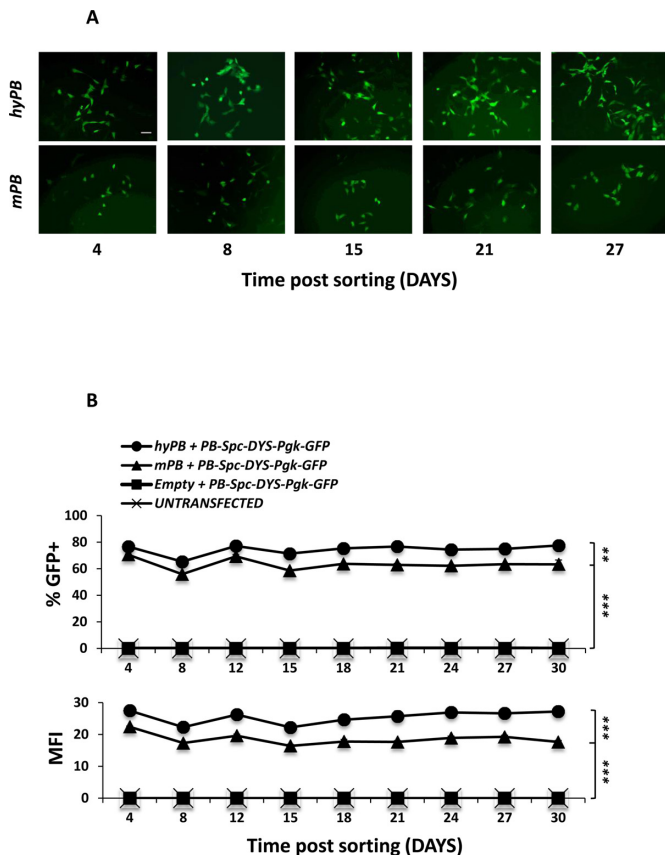


Figure 3. Validation of the use of *hyPB* transposase in C2C12 myoblasts. (A) Live cell imaging depicting the GFP expression in C2C12 myoblasts at different time points after sorting, when the large-size transposon *PB-SPc-DYS-Pgk-GFP* is co-transfected with *hyPB* or *mPB* transposase (Scale bar 100 μ m). (B) Graphs representing the comparison between *hyPB* and *mPB* transposases in terms of percentage of GFP+ population (graph above) and mean fluorescence intensity (MFI, graph below). The GFP+ populations were enriched by FACS at 4 days post-EP and monitored for the GFP expression in the next 30 days after the sorting. The higher efficiency of the *hyPB* transposase over the *mPB* transposase was assessed at the concentration of 0.32 pmol transposase DNA: 0.87 pmol transposon DNA. Results were presented as mean \pm SD of three independent biological replicates; two-way ANOVA (Bonferroni's multiple comparison test); *** $P \leq 0.001$; ** $P \leq 0.01$.

PB transposase and with the *PB-SPc-DYS-Pgk-GFP* transposon. Due to the large size transposon, the percentage of GFP positive C2C12 myoblasts at 4 days post-EP resulted to be $4 \pm 0.5\%$ after co-transfection with the *hyPB* transposase and $2 \pm 0.5\%$ after co-transfection with the *mPB* transposase. The GFP positive populations were then enriched by FACS sorting and monitored at different time points by FACS analysis and fluorescence microscopy (Figure 3A, B). At 30 days post sorting, $78 \pm 3\%$ of the cells transfected with the *hyPB* transposase were GFP positive, showing a statistically significant ($P \leq 0.01$) higher percentage compared to when the *mPB* was employed ($63 \pm 3\%$ GFP positive cells). Consistently, a statistically significant difference in MFI ($P \leq 0.001$) was detected by FACS when the *hyPB* was used compared to the *mPB* (Figure 3B).

We subsequently assessed whether C2C12 cells transposed with the *hyPB* transposase and the large-size trans-

poson *PB-SPc-DYS-Pgk-GFP* expressed the human full-length dystrophin and retained their ability to differentiate into skeletal muscle. Four days after incubation in the differentiation medium (corresponding to 24 days post-EP), multinucleated myotubes were observed. The transcription levels of the full-length human dystrophin were detectable by qRT-PCR and showed a significant increase in expression in C2C12 cells differentiated in myotubes compared to when the cells were retained in a proliferative, non-differentiated state ($P \leq 0.001$; Figure 4A). This is consistent with our previous results (Figure 2C, D) and confirms the muscle-specificity of the synthetic SPc5–12 promoter and its up-regulation upon myogenic differentiation. To demonstrate that the full-length human dystrophin *CDS* expresses a full-length transcript, a reverse transcriptase (RT)-PCR was first performed using three different primer pairs that respectively amplify three different regions of the full-length dystrophin transcript, including the N-terminal, central and C-terminal sequences (Supplementary data, Table S1). The three bands corresponding to these respective amplified regions were detected in differentiated C2C12 myoblasts that had undergone transposition after transfection with the *hyPB* transposase and the *PB-SPc-DYS-Pgk-GFP* transposon constructs (Figure 4B). In contrast, these specific PCR bands were absent in the untreated differentiated C2C12 cells or in differentiated C2C12 cells co-transfected with the *PB-SPc-DYS-Pgk-GFP* transposon and an empty expression plasmid without transposase (Figure 4B).

Western blot analysis subsequently confirmed expression of the full-length human dystrophin protein (427 kDa) in myotubes derived from C2C12 cells that had undergone transposition after transfection with the *hyPB* transposase and the *PB-SPc-DYS-Pgk-GFP* transposon constructs (Figure 4C). Dystrophin expression in these myotubes coincided with GFP and myosin expression, as confirmed by immunofluorescence (Figure 4D and E). Similarly, Western blot analysis demonstrated expression of the full-length human dystrophin protein (427 kDa) in differentiated normal human skeletal muscle cells (SKM, Figure 4C), whereas no dystrophin expression was apparent in non-transfected differentiated C2C12 cells or differentiated C2C12 cells co-transfected with the *PB-SPc-DYS-Pgk-GFP* transposon and an empty expression plasmid without transposase (Figure 4C).

Collectively, these results justify the use of hyperactive *PB* transposase to achieve a stable integration of the *PB* transposon encoding for the full-length human dystrophin and a sustained expression of the protein in differentiated myogenic cells.

Isolation and characterization of adult skeletal muscle pericyte-derived stem/progenitor cells from the Golden Retriever Muscular Dystrophy (GRMD) dog model

Adult pericyte-derived stem/progenitor cells or MABs were isolated from the skeletal muscle of a Golden Retriever Muscular Dystrophy (GRMD) dog, as previously described (45,53). Small, round, refractile and poorly adherent cells were visible with the initial outgrowth of adherent cells (Supplementary Figure S1A). This population of cells was collected, kept in culture and characterized for the typi-

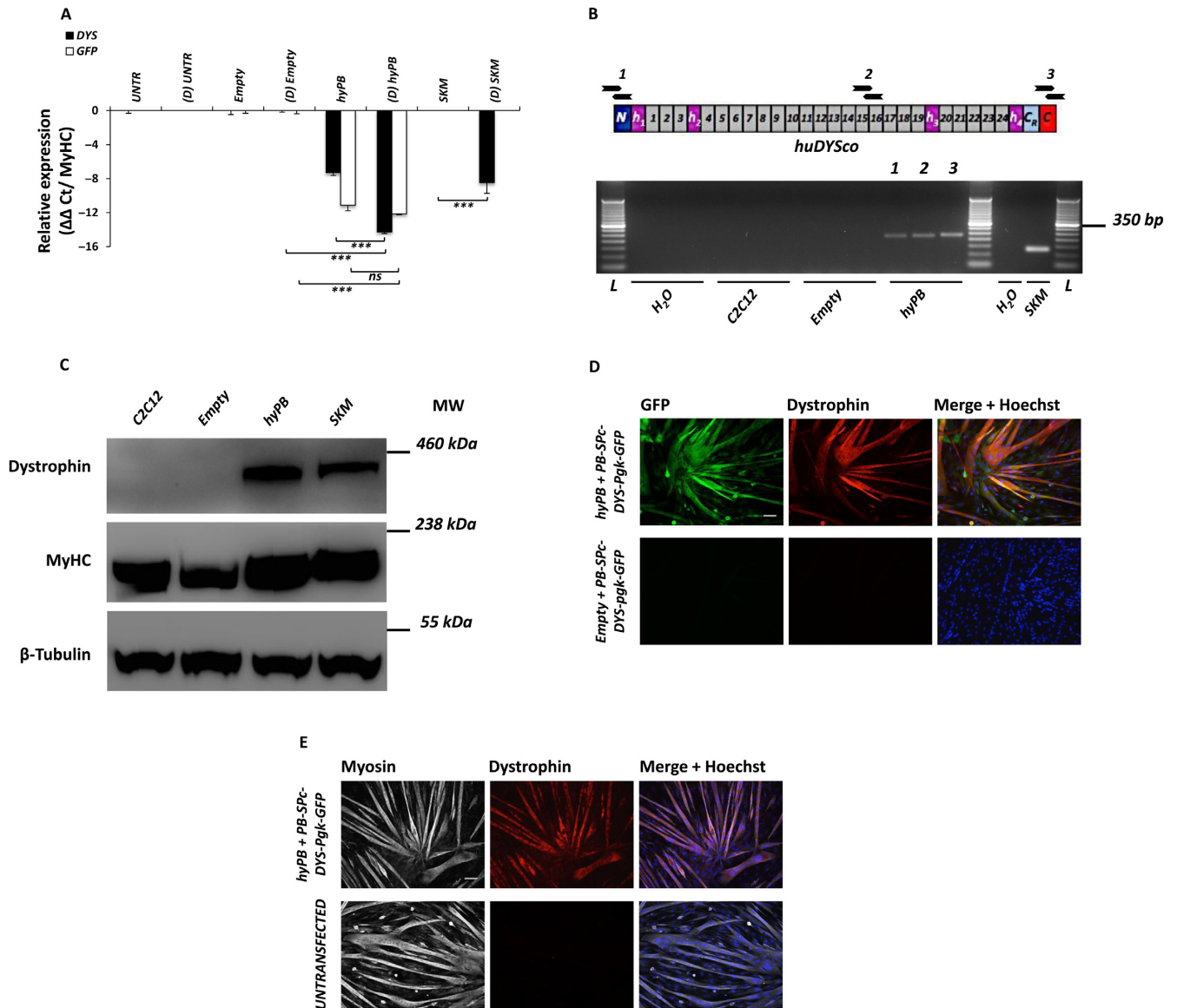


Figure 4. Human full-length dystrophin expression in *PB*-transposed C2C12 myoblast-derived differentiated myotubes. (A) The transcript levels of the full-length human dystrophin (black bars) and the GFP (white bars) were detected by qRT-PCR in C2C12 cells transposed with *hyPB + PB-SPc-DYS-Pgk-GFP*, while in proliferation or in differentiated myotubes (D: differentiated sample). Results were presented as mean±SEM of triplicate qRT-PCR analyses performed for three independent biological replicates; two-tailed unpaired Student's *t*-test (***) $P \leq 0.001$; ns: not significant). (B) RT-PCR showing expression of full-length human dystrophin transcript in myotubes derived from C2C12 cells that had undergone transposition after co-transfection with *hyPB* and *PB-SPc-DYS-Pgk-GFP*. Three different primer pairs were used that recognize respectively (1) the N-terminal, (2) a central region and (3) the C-terminal sequences, yielding amplicons of 221 bp, 222 bp and 228 bp, respectively. A schematic representation of the PCR primers relative to the different regions of the dystrophin transcript is depicted. Human skeletal muscle cells (SKM) differentiated in myotubes were used as a positive control. Negative controls included untreated differentiated C2C12 cells (designated as C2C12) or differentiated C2C12 cells co-transfected with the *PB-SPc-DYS-Pgk-GFP* transposon and an empty expression plasmid without transposase (designated as Empty). L: 50 bp ladder. (C) Western blot analysis demonstrating expression of the full-length human dystrophin protein (427 kDa) in myotubes derived from C2C12 cells that had undergone transposition after co-transfection with *hyPB* and *PB-SPc-DYS-Pgk-GFP*. The antibody NCL-DYS3 was used to detect the human dystrophin. Non-transfected differentiated C2C12 cells or differentiated C2C12 cells co-transfected with the *PB-SPc-DYS-Pgk-GFP* transposon and an empty expression plasmid without transposase were included as negative controls. Normal human skeletal muscle cells were used as positive control. *In vitro* skeletal muscle differentiation was confirmed for all the samples by the expression of the MyHC protein (223 kDa). β -Tubulin (50 kDa) was used to normalize the amount of loaded proteins. (D, E) Immunofluorescence staining on C2C12 myotubes upon 4 days in conditioning medium (24 days post-EP) C2C12 cells transposed with *hyPB + PB-SPc-DYS-Pgk-GFP* showed a co-localized expression of GFP (D, in green) and full-length human dystrophin (D, E in red) when differentiated in myotubes, as confirmed by the myosin expression (E, in white). The nuclei were stained with Hoechst (Scale bar 100 μ m). The Ab mouse anti-human dystrophin NCL-DYS3 was used.

cal markers of adult skeletal muscle MABs (43,53). Alkaline phosphatase (AP) positive cells were detected in the cultured cell population (Supplementary Figure S1B). The presence of the CD44 marker and the absence of CD34 and CD45 markers were assessed by FACS analyses, showing the typical profile of this subset of adult pericytes (Supplementary Figure S1C). Further markers were subsequently analyzed by semi-quantitative RT-PCR at different time points (passage P5 and P10), using as a positive control a heterogeneous bulk cell population directly derived from the GRMD muscle biopsy (passage P1). As expected, the transcript levels of *PAX7*, *MYF5*, *CD56* and desmin, typically associated with satellite cells, decreased significantly after the first passage ($P \leq 0.01$, $P \leq 0.001$; Supplementary Figure S1D, SE). In contrast, the transcript levels of *NG2* and *PDGFR β* , typical markers of pericytes, remained stable over time. Finally, the isolated cell population was capable to spontaneously differentiate *in vitro* into skeletal myotubes or into mesodermal lineages upon appropriated stimulation (Supplementary Figure S1F, SG). Collectively, this gene expression profile and functional analyses confirmed that the GRMD cell isolated were *bona fide* MABs.

Genetic correction of dystrophic mesoangioblasts by delivery of the full-length human dystrophin CDS in *PB* transposon system

We subsequently optimized the transfection conditions of the dystrophic GRMD MABs. These were transfected by electroporation with the *hyPB* transposase-encoding construct and the *PB-Pgk-GFP* transposon (ratio of 0.32 pmol transposase DNA: 0.87 pmol transposon DNA) showing a transfection efficiency of $44 \pm 1\%$ GFP+ cells at 7 days post-EP (Figure 5A). The transfected cells were sorted and the GFP expression was maintained, resulting in $88 \pm 3\%$ GFP+ cells at 28 days post sorting ($P \leq 0.001$; Figure 5B). In contrast, in the absence of the *hyPB* transposase, the percentage of GFP+ cells gradually declined resulting in only background levels of GFP, indistinguishable from untransfected control GRMD MABs (Figure 5B). This indicates that the sustained GFP expression in the transfected MABs could be ascribed to and is dependent on *bona fide* transposition. Based on these encouraging results, we subsequently transfected the GRMD MABs by electroporation with the same molar ratios of *hyPB* transposase expression construct and the large-size transposon *PB-SPc-DYS-Pgk-GFP* (ratio of 0.32 pmol transposase DNA: 0.87 pmol transposon DNA), encoding both full-length human dystrophin and GFP. This resulted in a transfection efficiency of $3 \pm 1\%$ GFP+ cells at 7 days post-EP (Figure 5A). The difference in transfection efficiency between the equimolar doses of *PB-SPc-DYS-Pgk-GFP* and *PB-Pgk-GFP* transposons reflected the different sizes of the plasmids, as previously reported ($P \leq 0.001$, Figure 5A) (66). Though doubling the *hyPB* transposase and transposon doses, while maintaining the transposase: transposon ratio, further increased the percentage of GFP+ cells (Supplementary Figure S2), the viability of the transfected cells concomitantly declined ($P \leq 0.001$). GRMD MABs transfected with *hyPB* transposase and *PB-SPc-DYS-Pgk-GFP* transposon were sorted at 7 days post-EP, and the GFP expression was monitored

by FACS analysis and fluorescence microscopy during the 28 days post sorting (Figure 5B, C). The transfected cells exhibited stable expression of $50 \pm 5\%$ GFP+ cells, consistent with stable transposition ($P \leq 0.001$). The transposon copies per diploid genome quantified by qPCR corresponded to 0.5 ± 0.03 copies for the condition *hyPB* + *PB-SPc-DYS-Pgk-GFP* and 1.7 ± 0.04 copies for *hyPB* + *PB-Pgk-GFP* (Figure 5D). GRMD MABs that were transfected with the transposon and without the transposase did not show any detectable integrated transposons ($P \leq 0.001$), indistinguishable from non-transfected control cells.

To assess if the integrated *PB-SPc-DYS-Pgk-GFP* transposon could result in sustained expression of the full-length human dystrophin, transposed GRMD MABs were subsequently differentiated *in vitro* into myocytes/myotubes after tamoxifen-induced overexpression of MyoD-ER (61). This approach allowed to rescue myogenic differentiation of adult canine MABs at late passages (i.e. passage P15–18). The transcript levels of the full-length human dystrophin were detected by qRT-PCR ($P \leq 0.001$; Figure 6A). Moreover, the three different regions including the N-terminal, the central region and the C-terminal region of the full-length human dystrophin transcript were detected by RT-PCR in the differentiated GRMD MABs that had undergone transposition after transfection with the *hyPB* transposase and the *PB-SPc-DYS-Pgk-GFP* transposon constructs (Figure 6B). The expression of the full-length human dystrophin protein was confirmed by immunofluorescence in differentiated GRMD MABs, where it co-localized with the expression of GFP (Figure 6C) and myosin (Figure 6D) in genetically corrected myocytes/myotubes. In contrast, dystrophin and GFP were not detectable in untransfected cells nor in the control GRMD MABs co-transfected with the *PB-SPc-DYS-Pgk-GFP* transposon and the empty expression plasmid without transposase (Figure 6C, D). This was consistent with the lack of dystrophin mRNA in these controls (Figure 6A, B). Similarly, sustained GFP transcript levels were detected by qRT-PCR in GRMD MABs that had undergone transposition after co-transfection with *hyPB* transposase and *PB-Pgk-GFP* transposon ($P \leq 0.001$; Figure 6A). The GFP expression was confirmed by IF in differentiated cells (Supplementary Figure S3). In the absence of the *hyPB* transposase, GFP transcript and protein were absent, confirming the need for transposition to enable stable integration and transgene expression (Figure 6A, Supplementary Figure S3).

Taken together, these findings demonstrate that it is possible to genetically correct dystrophic adult mesoangioblasts by using a *PB*-transposon based platform to deliver the full-length human dystrophin *CDS*.

DISCUSSION

In this study, we demonstrated that the *PB* transposon platform could be used to obtain stable expression of a therapeutically relevant, large-sized transgene such as the human full-length dystrophin coding DNA sequence (*CDS*), leading to the correction of dystrophic myogenic stem/progenitor cells derived from a dystrophic large animal model. Recent studies have tried to explore the use of transposons to investigate therapeutic strategies in mus-

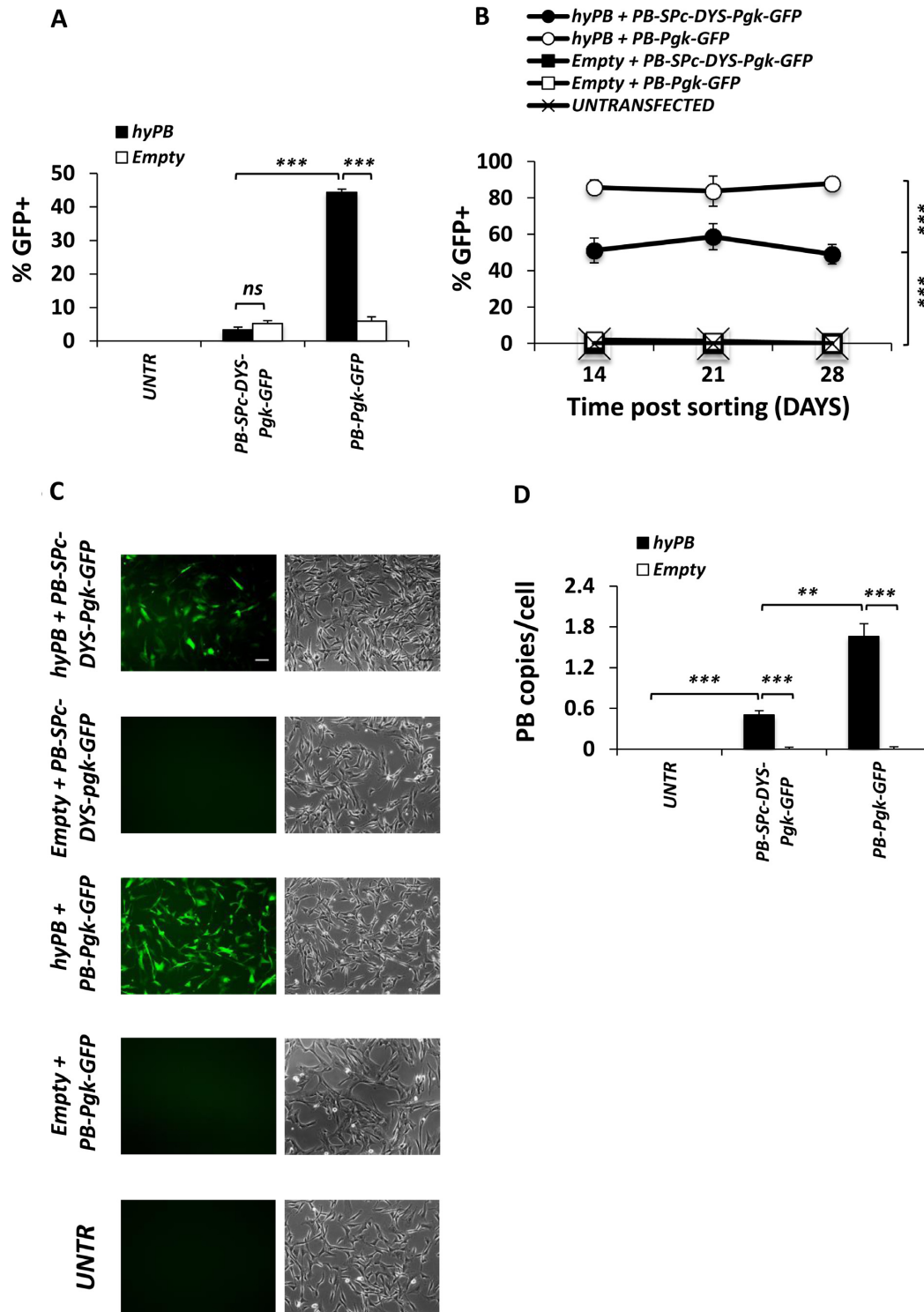


Figure 5. PB-mediated transposition of the full-length human dystrophin *CDS* in GRMD MABs. (A) The bar graph shows the percentage of GFP+ GRMD MABs at the day of the sorting performed at 7 days post-EP. Optimized and equimolar doses have been used in the different conditions. The statistically significant difference in transfection efficiency detected when *PB-SPc-DYS-Pgk-GFP* or *PB-Pgk-GFP* transposon are deployed reflects the different sizes of the plasmids. Results were presented as mean±SEM of three independent biological replicates; two-tailed unpaired Student's *t*-test ($***P \leq 0.001$; ns: not significant). (B) The GFP+ populations were monitored at different time points for 28 days post sorting. GRMD MABs co-transfected with the empty plasmid and the same transposons, and untransfected cells were used as controls. Shown are mean±SD on a biological replicate; two-way ANOVA (Bonferroni's multiple comparison test); $***P \leq 0.001$. (C) Live cell imaging showing the GFP expression of the different conditions at day 21 post sorting (Scale bar 100 μ m). (D) Bar graph representing the transposon copies per diploid genome detected by qPCR in transposed GRMD MABs (*PB-SPc-DYS-Pgk-GFP* 0.5 ± 0.03 copies/cell; *PB-Pgk-GFP* 1.7 ± 0.04 copies/cell). Shown are mean±SEM of triplicate qRT-PCR analyses performed for a biological replicate; two-tailed unpaired Student's *t*-test ($***P \leq 0.001$; $**P \leq 0.01$).

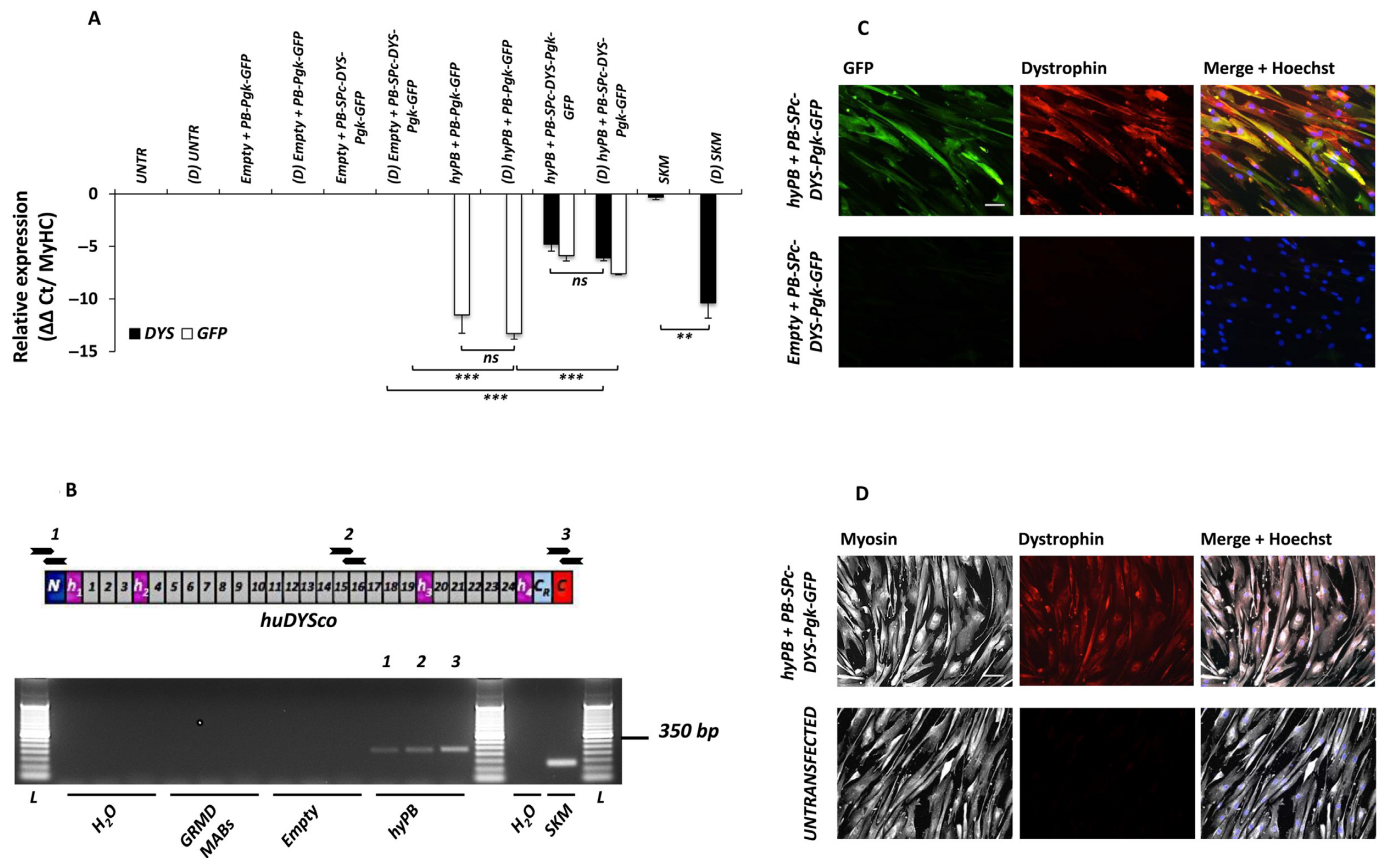


Figure 6. Correction of GRMD MABs by the *PB*-mediated expression of the full-length human dystrophin. (A) The transcript levels of the full-length human dystrophin (black bars) and GFP (white bars) were detected by qRT-PCR analysis in GRMD MABs transfected with *hyPB* + *PB-SPc-DYS-Pgk-GFP* or *PB-Pgk-GFP*. SKM cells have been used as positive control. Samples are indicated with (D) when differentiated in myocytes/myotubes. Results were presented as mean \pm SEM of triplicate qRT-PCR analyses performed for a biological replicate; two-tailed unpaired Student's *t*-test (** $P \leq 0.01$; *** $P \leq 0.001$; ns: not significant; D: differentiated sample). (B) RT-PCR demonstrating expression of full-length human dystrophin transcript in differentiated GRMD MABs that had undergone transposition after co-transfection with *hyPB* and *PB-SPc-DYS-Pgk-GFP*. Three different primer pairs were used that recognize respectively (1) the N-terminal, (2) a central region and (3) the C-terminal sequences, yielding amplicons of 221 bp, 222 bp and 228 bp, respectively. A schematic representation of the PCR primers relative to the different regions of the dystrophin transcript is depicted. Controls included differentiated human SKM, untreated differentiated MABs (designated as GRMD MABs) and differentiated GRMD MABs co-transfected with the *PB-SPc-DYS-Pgk-GFP* transposon and an empty expression plasmid without transposase (designated as Empty). L: 50 bp ladder. (C,D) At 21 days post-EP, GRMD MABs corrected with *hyPB* + *PB-SPc-DYS-Pgk-GFP* were induced to differentiate in skeletal muscle *in vitro* upon MyoD-ER overexpression and 6 days in conditioning medium. Immunofluorescence analysis confirms the expression and co-localization of the full-length human dystrophin (C, D in red) with the GFP (C, in green), or with the myosin (D, in white). The conditions empty plasmid + *PB-SPc-DYS-Pgk-GFP* as well as the untransfected cells are also shown as negative controls. The nuclei were stained with Hoechst (Scale bar 100 μ m). The mouse anti-dystrophin NCL-DYS1 and NCL-DYS2 antibodies were used.

cular dystrophies, but they were limited to the use of reporter or marker genes (67–69), truncated versions of either dystrophin or utrophin (70,71) or conditionally immortalized muscle cell-derived cell-lines (67,70), that cannot be deployed clinically. To our knowledge, this is the first report that establishes the use of *PB* transposons encoding for the full-length human dystrophin enabling genetic correction of dystrophic primary cells. This represents a proof of concept study toward the development of a novel stem cell-based gene therapy approach for Duchenne muscular dystrophy with potentially broad implications for the field at large.

The main advantage of *PB* transposons is that they efficiently integrate their cargo into the target cell genome. This property enables robust stable gene expression in both human and mouse cells, *ex vivo* or *in vivo* (33,37–39,54,60,72). This attribute is particularly relevant for stable genetic

modification of stem/progenitor cells, given their intrinsic self-renewal and differentiation potential (73). As we observed in this study, *PB* transposons can integrate and provide dystrophin expression in dystrophic mesoangioblasts (MABs) and their differentiated progeny. In contrast, only transient or no expression was observed in the absence of any transposase-encoding construct. This indicates that *bona fide* transposition was a prerequisite for a robust dystrophin expression in dystrophic MABs. It is known, indeed, that transfection of conventional plasmids results in a very low stable integration frequency (typically 1 stable integrant per 10^5 transfected cells) (60) that consequently hampers potential clinical applications. The efficiency of *PB* transposon-mediated delivery of the full-length human dystrophin *CDS* compares favorably with alternative approaches that allowed the production of the wild-type full

length dystrophin protein, such as the human artificial chromosome (HAC; (74,75)). This vector is recognized as an endogenous chromosome within the host cells and is stably maintained throughout subsequent cell divisions obviating the need for genomic integration. The entire human dystrophin genomic locus (2.4 Mb), including the native promoter and regulatory elements, has been accommodated into the HAC (76,77) and transferred in dystrophic murine mesoangioblasts and DMD patient specific human iPSC-derived mesoangioblast-like cells (47,78). This approach resulted in the full-length human dystrophin expression in genetically corrected cells. Nevertheless, the generation of such a relatively complex vector like the HAC, together with the low efficiency of microcell-mediated chromosome transfer (MMCT; approximately 1.2×10^{-5}) required to introduce HACs into the target cells, may limit the application of this technology only to clonogenic stem/progenitor cells with high proliferation potential. On the other hand, the use of *PB* transposons is at least 10^4 -fold more efficient than MMCT and may ease the manufacturing constraints compared to MMCT or viral vectors, ultimately facilitating ultimate clinical translation of the *PB* transposon vectors.

Another advantage of the *PB* transposons is that they enabled stable delivery of the full-length human dystrophin *CDS* together with a reporter marker (insert size: 13.7 kb). This exceeds the packaging capacity of γ -retroviral and lentiviral vectors (<10 kb) and AAV vectors (5 kb). Consequently, this obviates concerns associated with the use of truncated dystrophins that may not replicate all of the necessary functions of its wild-type counterpart (45). Moreover, expression of full-length human dystrophin is broadly applicable to all patients suffering from DMD, regardless of the underlying genetic defect in the dystrophin locus. This is in contrast with other approaches that are restricted in their application to correcting specific mutations of the gene, such as exon-skipping strategies (18,79,80) or the use of engineered nucleases (81–83). The ability of *PB* transposons to deliver such a relatively large cargo is consistent with previous reports indicating that *PB* transposons can mediate the transfer of large genetic cargos up to 100 kb (32,33). The availability of *PB* transposons encoding either full-length or truncated dystrophin *CDS* characterized in this study may pave the way toward future comprehensive structure-function and comparative studies. Indeed, the present study has broader implications for the use of other hyperactive transposon systems, such as *Sleeping Beauty* for gene therapy of DMD (84–86).

In the present study, we have used nucleofection technology, an electroporation-based transfection method that allows to transfer the DNA plasmids directly into the nuclei and the cytoplasm of both dividing and non-dividing cells *in vitro*. This technique overcomes the limitations related to other transfection methods that rely on nuclear import of plasmid DNA in non-dividing cells (i.e. polycations). However, large-size DNA plasmids adversely impact on the transfection efficiency (66). In accordance with these previous findings, we showed that the use of large transgenes (e.g. full-length human dystrophin *CDS* as opposed to truncated MD1 and MD2 human microdystrophin *CDS*) and/or increasing DNA concentrations resulted in a net decrease in transfection efficiency. This may be due, at

least in part, by the intrinsic property of the DNA plasmids such as the presence of unmethylated CpG motifs in the backbone sequences that might impair cell viability, possibly involving Toll-like receptor (TLR) pathways (87,88). Indeed, plasmids with a low content in CpG motifs confer long-term gene expression with less toxicity (89,90). Alternatively, transfection efficiency may also have been affected by nuclear import of plasmid DNA in non-dividing cells and/or reduced cytosolic mobility of large size plasmid DNA (91). Nevertheless, the surviving transfected cells could be easily enriched by FACS sorting yielding more than 50% MABs that had undergone stable transposition. Moreover, we demonstrated that the use of the hyperactive *PB* transposase (37) compared to the native *PB* transposase (92) can boost the efficiency and stable expression of large-size transposons, allowing the use of lower amounts of DNA plasmids, and consequently reducing overall DNA toxicity in the transfected cells. Nevertheless, it may be worthwhile to further explore alternative strategies to augment the overall transfection efficiency, viability and expression of the therapeutic gene. This could potentially be achieved by using a minicircle-based transposon system, devoid of any bacterial backbone sequence, as recently validated for *Sleeping Beauty* (66). Consequently, this would reduce the plasmid size, lower CpG content, increase transfection efficiency and decrease DNA toxicity. Alternatively, more potent muscle-specific promoters could be used to drive expression of the full-length dystrophin *CDS*.

Though the genomic integration of the *PB* transposons is required for sustained expression in dividing and differentiating stem/progenitor cells, it could raise some concerns related to the risk of insertional oncogenesis by potentially activating oncogenes that are in the vicinity of the integration sites (93). *PB* transposons exhibit a random integration pattern in the genome of murine mesoangioblasts suggesting that they do not preferentially integrate into genes and their regulatory regions (69). This risk of insertional oncogenesis could be minimized further by retargeting *PB*-mediated integration into potential 'safe harbor' loci (94,95). However, it is reassuring that the *PB* transposon copy number detected in the present study fell within an acceptable and relatively safe range of genomic integrations per cell (i.e. 0.5–1.7 copies per diploid genome), in accordance with the European medicines agency guidelines (http://www.ema.europa.eu/ema/index.jsp?curl=pages/regulation/general/general_content_000410.jsp&mid=WC0b01ac058002958d).

The therapeutic relevance of MABs, even after prolonged *in vitro* culture, has been highlighted in many previous studies (44–48). Their intrinsic capability to cross the wall vessels when injected intra-arterially and to contribute to the muscle regeneration in animal models has represented a substantial advantage over other muscle stem cells (i.e. myoblasts) (42). We have confirmed the characteristic phenotype of the MABs used in our current study based on the expression of MAB markers (Supplementary Figure S1) and their ability to undergo myogenic differentiation *in vitro* (Supplementary Figures S1 and S3, Figure 6). According to previous and recent studies on human MABs, a high proliferation rate has been observed for approximately 20 population doublings, with a doubling time of approximately

36 h (42,49) without compromising their stem cell properties. Though the initial transfection efficiency in MABs was about 3%, we could rapidly enrich for those cells that had undergone stable transposition by FACS sorting, thus avoiding protracted cell culture.

Dystrophin levels corresponding to 30% of the levels normally found in healthy individuals and in animal models are sufficient to prevent muscular dystrophy (96,97). In accordance with these data, pre-clinical studies based on the use of MABs have shown a therapeutic effect in dystrophic mice and dogs with dystrophin expression ranging 20 to 30% of normal levels (45,47). This has typically been achieved by injecting 5×10^7 cells/kg in the dog model. Considering treatment of pediatric subjects with less advanced muscle disease and more likely to benefit from this cell therapy, this would translate into a total cell dose of 75×10^7 MABs in a 15 kg patient although the possibility of repeated injection to reach efficacy still needs to be investigated. Up to 2×10^9 human MABs can readily be obtained after *in vitro* expansion of initial cells isolated from a single muscle biopsy (100–200 mg) (42,49). Based on our current results, we estimated that 9×10^8 stably transfected MABs expressing dystrophin after *PB*-mediated transposition could be obtained 35 days post-transfection of 3×10^6 cells. Consequently, the required dose to treat pediatric DMD patients is within reach. It is encouraging that initially more MABs outgrew from explants of young DMD patients (42) suggesting that the yield of MABs and/or their proliferative capacity may possibly be even higher in younger than in older patients with advanced disease.

Allogeneic MABs have recently been tested in a first-in-human phase I/II clinical trial in DMD patients under immunosuppressive treatment (EudraCT N° 2011–000176–33, (49)). Administration at escalating doses of HLA-matched donor MABs in the limb arteries of the patients was considered relatively safe, which was the primary endpoint of the study. One patient developed an acute thalamic stroke with no clinical consequences but it was unclear whether it correlated with the MAB infusion. Muscle biopsies confirmed the presence of donor DNA in 4/5 patients and expression of donor dystrophin in one patient. Though no functional improvements were observed in the treated patients, functional measures appeared to be stabilized in 2/3 ambulant patients. The study also provided insights to further improve efficacy by enrolling younger patients with less advanced muscle disease and/or increase the MAB dose. Moreover, the use of gene-modified autologous MABs may further augment the efficacy with the added advantage over allogeneic MABs that immune suppression may not be needed in this case.

Though MABs can be expanded extensively for 20 passages and exhibit a remarkable proliferative potential, their lifespan is limited nonetheless (53). This likely reflected normal cellular processes that gradually contribute to cellular senescence (98). Nevertheless, this did not preclude clinical translation (49). In addition, the *PB* transposon technology is potentially amenable to be used in alternative adult myogenic stem cell sources distinct from MABs (99,100). Ultimately, the use of iPSC-derived myogenic cells, that have unlimited expansion potential, may represent an attractive alternative, provided they can safely and efficiently be con-

verted into transplantable myogenic cells (71,78,101–103). In a separate study (Loperfido *et al.*, unpublished observations), we genetically corrected DMD patient-specific iPSC-derived myogenic cells with the same *PB* transposon encoding for the full-length human dystrophin and transplanted the engineered cells in SCID/mdx mice. Dystrophin expression could be detected *in vitro* and *in vivo* by immunofluorescence on the fiber membrane of the transplanted muscles.

In conclusion, this study provides the first evidence of *PB*-mediated human full-length dystrophin expression in dystrophic MABs for the treatment DMD. Further characterizations *in vivo* are needed upon transplantation of the *PB* transposon-modified MABs in the GRMD model, to ultimately justify a clinical study in patients suffering from DMD.

SUPPLEMENTARY DATA

Supplementary Data are available at NAR Online.

ACKNOWLEDGEMENT

We thank Dr Chrystelle Richard from Le Centre de Boisbonne- ONIRIS (Nantes-Atlantique, France) to kindly provide the skeletal muscle biopsies from Golden Retriever muscular dystrophy dogs. We also thank Petra Vandervoort and Boukje Hoekman (FACS Core, KUL), Angelo Willems (Cytometry Core Unit, VUB) and Abel Acosta-Sanchez for technical assistance.

FUNDING

Fonds voor Wetenschappelijk Onderzoek (Flanders Fund for Scientific Research; FWO) [FWO G.0960.11 to T.V., FWO G.0763.10 to M.K.C.]; ‘Aspirant’ Fonds voor Wetenschappelijk Onderzoek (‘Research Fellowship of the Flanders Fund for Scientific Research’; FWO to M.L. and M.D.M.); Wetenschappelijk Fonds Willy Gepts (Willy Gepts Fund, VUB) to ML; Association Française contre les Myopathies (AFM), EU Framework Program 6 (CliniGene) and Walter Peleman Fund (King Boudewijn Foundation) to T.V. and M.K.C; Funds from the Muscular Dystrophy United Kingdom, Association Monegasques contre les Myopathies and the EU-FP7 (to G.D., S.A.J., M.M. and T.A.); Agentschap voor Innovatie door Wetenschap en Technological (Doctoral Grant for Strategic Basic Research; IWT to S.A.J., M.M. and T.A). Funding for open access charge: Fonds voor Wetenschappelijk Onderzoek.

Conflict of interest statement. Authors declare having no potential competing financial interests related to the technologies described in this study.

REFERENCES

- Mendell, J.R. and Lloyd-Puryear, M. (2013) Report of MDA muscle disease symposium on newborn screening for Duchenne muscular dystrophy. *Muscle Nerve*, **48**, 21–26.
- Hoffman, E.P., Brown, R.H. and Kunkel, L.M. (1987) Dystrophin: the protein product of the Duchenne muscular dystrophy locus. *Cell*, **51**, 919–928.
- Bonilla, E., Samitt, C.E., Miranda, A.F., Hays, A.P., Salviati, G., DiMauro, S., Kunkel, L.M., Hoffman, E.P. and Rowland, L.P. (1988) Duchenne muscular dystrophy: deficiency of dystrophin at the muscle cell surface. *Cell*, **54**, 447–452.

4. Ervasti, J.M. (2007) Dystrophin, its interactions with other proteins, and implications for muscular dystrophy. *Biochim. Biophys. Acta*, **1772**, 108–117.
5. Mercuri, E. and Muntoni, F. (2013) Muscular dystrophies. *Lancet*, **381**, 845–860.
6. Bushby, K., Finkel, R., Birnkrant, D.J., Case, L.E., Clemens, P.R., Cripe, L., Kaul, A., Kinnett, K., McDonald, C., Pandya, S. *et al.* (2010) Diagnosis and management of Duchenne muscular dystrophy, part 1: diagnosis, and pharmacological and psychosocial management. *Lancet Neurol.*, **9**, 77–93.
7. Bushby, K., Finkel, R., Birnkrant, D.J., Case, L.E., Clemens, P.R., Cripe, L., Kaul, A., Kinnett, K., McDonald, C., Pandya, S. *et al.* (2010) Diagnosis and management of Duchenne muscular dystrophy, part 2: implementation of multidisciplinary care. *Lancet Neurol.*, **9**, 177–189.
8. Serra, F., Quarta, M., Canato, M., Toniolo, L., De Arcangelis, V., Trotta, A., Spath, L., Monaco, L., Reggiani, C. and Naro, F. (2012) Inflammation in muscular dystrophy and the beneficial effects of non-steroidal anti-inflammatory drugs. *Muscle Nerve*, **46**, 773–784.
9. Mercuri, E. and Muntoni, F. (2015) Efficacy of idebenone in Duchenne muscular dystrophy. *Lancet*, **385**, 1704–1706.
10. Benedetti, S., Hoshiya, H. and Tedesco, F.S. (2013) Repair or replace? Exploiting novel gene and cell therapy strategies for muscular dystrophies. *FEBS J.*, **280**, 4263–4280.
11. Seto, J.T., Bengtsson, N.E. and Chamberlain, J.S. (2014) Therapy of genetic disorders—novel therapies for Duchenne muscular dystrophy. *Curr. Pediatr. Rep.*, **2**, 102–112.
12. Aartsma-Rus, A. (2010) Antisense-mediated modulation of splicing: therapeutic implications for Duchenne muscular dystrophy. *RNA Biol.*, **7**, 453–461.
13. Mendell, J.R., Rodino-Klapac, L.R., Sahenk, Z., Roush, K., Bird, L., Lowes, L.P., Alfano, L., Gomez, A.M., Lewis, S., Kota, J. *et al.* (2013) Eteplirsen for the treatment of Duchenne muscular dystrophy. *Ann. Neurol.*, **74**, 637–647.
14. Emery, A.E.H. (2002) The muscular dystrophies. *Lancet*, **359**, 687–695.
15. Helderman-van den Enden, A.T.J.M., Straathof, C.S.M., Aartsma-Rus, A., den Dunnen, J.T., Verbist, B.M., Bakker, E., Verschuuren, J.J.G.M. and Ginjaar, H.B. (2010) Becker muscular dystrophy patients with deletions around exon 51: a promising outlook for exon skipping therapy in Duchenne patients. *Neuromuscul. Disord.*, **20**, 251–254.
16. van den Bergen, J.C., Schade van Westrum, S.M., Dekker, L., van der Kooi, A.J., de Visser, M., Wokke, B.H.A., Straathof, C.S., Hulsker, M.A., Aartsma-Rus, A., Verschuuren, J.J. *et al.* (2014) Clinical characterisation of Becker muscular dystrophy patients predicts favourable outcome in exon-skipping therapy. *J. Neurol. Neurosurg. Psychiatry*, **85**, 92–98.
17. Findlay, A.R., Wein, N., Kaminoh, Y., Taylor, L.E., Dunn, D.M., Mendell, J.R., King, W.M., Pestronk, A., Florence, J.M., Mathews, K.D. *et al.* (2015) Clinical phenotypes as predictors of the outcome of skipping around DMD exon 45. *Ann. Neurol.*, **77**, 668–674.
18. Lu, Q.-L., Cirak, S. and Partridge, T. (2014) What can we learn from clinical trials of exon skipping for DMD? *Mol. Ther. Nucleic Acids*, **3**, e152.
19. Koenig, M., Hoffman, E.P., Bertelson, C.J., Monaco, A.P., Feener, C. and Kunkel, L.M. (1987) Complete cloning of the Duchenne muscular dystrophy (DMD) cDNA and preliminary genomic organization of the DMD gene in normal and affected individuals. *Cell*, **50**, 509–517.
20. Muntoni, F., Torelli, S. and Ferlini, A. (2003) Dystrophin and mutations: one gene, several proteins, multiple phenotypes. *Lancet Neurol.*, **2**, 731–740.
21. Kawano, R., Ishizaki, M., Maeda, Y., Uchida, Y., Kimura, E. and Uchino, M. (2008) Transduction of full-length dystrophin to multiple skeletal muscles improves motor performance and life span in utrophin/dystrophin double knockout mice. *Mol. Ther.*, **16**, 825–831.
22. Guse, K., Suzuki, M., Sule, G., Bertin, T.K., Tyynismaa, H., Ahola-Erkkilä, S., Palmer, D., Suomalainen, A., Ng, P., Cerullo, V. *et al.* (2012) Capsid-modified adenoviral vectors for improved muscle-directed gene therapy. *Hum. Gene Ther.*, **23**, 1065–1070.
23. Gregorevic, P., Blankinship, M.J., Allen, J.M., Crawford, R.W., Meuse, L., Miller, D.G., Russell, D.W. and Chamberlain, J.S. (2004) Systemic delivery of genes to striated muscles using adeno-associated viral vectors. *Nat. Med.*, **10**, 828–834.
24. Gregorevic, P., Allen, J.M., Minami, E., Blankinship, M.J., Haraguchi, M., Meuse, L., Finn, E., Adams, M.E., Froehner, S.C., Murry, C.E. *et al.* (2006) rAAV6-microdystrophin preserves muscle function and extends lifespan in severely dystrophic mice. *Nat. Med.*, **12**, 787–789.
25. Koppanati, B.M., Li, J., Xiao, X. and Clemens, P.R. (2009) Systemic delivery of AAV8 in utero results in gene expression in diaphragm and limb muscle: treatment implications for muscle disorders. *Gene Ther.*, **16**, 1130–1137.
26. Rodino-Klapac, L.R., Montgomery, C.L., Bremer, W.G., Shontz, K.M., Malik, V., Davis, N., Sprinkle, S., Campbell, K.J., Sahenk, Z., Clark, K.R. *et al.* (2010) Persistent expression of FLAG-tagged micro dystrophin in nonhuman primates following intramuscular and vascular delivery. *Mol. Ther.*, **18**, 109–117.
27. Brunetti-Pierri, N., Palmer, D.J., Beaudet, A.L., Carey, K.D., Finegold, M. and Ng, P. (2004) Acute toxicity after high-dose systemic injection of helper-dependent adenoviral vectors into nonhuman primates. *Hum. Gene Ther.*, **15**, 35–46.
28. Wang, Z., Kuhr, C.S., Allen, J.M., Blankinship, M., Gregorevic, P., Chamberlain, J.S., Tapscott, S.J. and Storb, R. (2007) Sustained AAV-mediated dystrophin expression in a canine model of Duchenne muscular dystrophy with a brief course of immunosuppression. *Mol. Ther.*, **15**, 1160–1166.
29. Mingozzi, F., Meulenberg, J.J., Hui, D.J., Basner-Tschakarjan, E., Hasbrouck, N.C., Edmonson, S.A., Hutnick, N.A., Betts, M.R., Kastelein, J.J., Stroes, E.S. *et al.* (2009) AAV-1-mediated gene transfer to skeletal muscle in humans results in dose-dependent activation of capsid-specific T cells. *Blood*, **114**, 2077–2086.
30. Wang, Z., Halbert, C.L., Lee, D., Butts, T., Tapscott, S.J., Storb, R. and Miller, A.D. (2014) Elimination of contaminating cap genes in AAV vector virions reduces immune responses and improves transgene expression in a canine gene therapy model. *Gene Ther.*, **21**, 363–370.
31. Wu, S.C.-Y., Meir, Y.-J.J., Coates, C.J., Handler, A.M., Pelczar, P., Moisyadi, S. and Kaminski, J.M. (2006) piggyBac is a flexible and highly active transposon as compared to sleeping beauty, Tol2, and Mos1 in mammalian cells. *Proc. Natl. Acad. Sci. U.S.A.*, **103**, 15008–15013.
32. Li, M.A., Turner, D.J., Ning, Z., Yusa, K., Liang, Q., Eckert, S., Rad, L., Fitzgerald, T.W., Craig, N.L. and Bradley, A. (2011) Mobilization of giant piggyBac transposons in the mouse genome. *Nucleic Acids Res.*, **39**, e148.
33. Ding, S., Wu, X., Li, G., Han, M., Zhuang, Y. and Xu, T. (2005) Efficient transposition of the piggyBac (PB) transposon in mammalian cells and mice. *Cell*, **122**, 473–483.
34. Fraser, M.J., Brusca, J.S., Smith, G.E. and Summers, M.D. (1985) Transposon-mediated mutagenesis of a baculovirus. *Virology*, **145**, 356–361.
35. Cary, L.C., Goebel, M., Corsaro, B.G., Wang, H.G., Rosen, E. and Fraser, M.J. (1989) Transposon mutagenesis of baculoviruses: analysis of Trichoplusia ni transposon IFP2 insertions within the FP-locus of nuclear polyhedrosis viruses. *Virology*, **172**, 156–169.
36. Wilson, M.H., Coates, C.J. and George, A.L. (2007) PiggyBac transposon-mediated gene transfer in human cells. *Mol. Ther.*, **15**, 139–145.
37. Yusa, K., Zhou, L., Li, M.A., Bradley, A. and Craig, N.L. (2011) A hyperactive piggyBac transposase for mammalian applications. *Proc. Natl. Acad. Sci. U.S.A.*, **108**, 1531–1536.
38. Doherty, J.E., Huye, L.E., Yusa, K., Zhou, L., Craig, N.L. and Wilson, M.H. (2012) Hyperactive piggyBac gene transfer in human cells and in vivo. *Hum. Gene Ther.*, **23**, 311–320.
39. Di Matteo, M., Belay, E., Chuah, M.K. and Vandendriessche, T. (2012) Recent developments in transposon-mediated gene therapy. *Expert Opin. Biol. Ther.*, **12**, 841–858.
40. Mitra, R., Fain-Thornton, J. and Craig, N.L. (2008) piggyBac can bypass DNA synthesis during cut and paste transposition. *EMBO J.*, **27**, 1097–1109.
41. Minasi, M.G., Riminucci, M., De Angelis, L., Borello, U., Berarducci, B., Innocenzi, A., Caprioli, A., Sirabella, D., Baiocchi, M., De Maria, R. *et al.* (2002) The meso-angioblast: a multipotent, self-renewing cell that originates from the dorsal aorta and

- differentiates into most mesodermal tissues. *Development*, **129**, 2773–2783.
42. Dellavalle, A., Sampaolesi, M., Tonlorenzi, R., Tagliafico, E., Sacchetti, B., Perani, L., Innocenzi, A., Galvez, B.G., Messina, G., Morosetti, R. *et al.* (2007) Pericytes of human skeletal muscle are myogenic precursors distinct from satellite cells. *Nat. Cell Biol.*, **9**, 255–267.
 43. Dellavalle, A., Maroli, G., Covarello, D., Azzoni, E., Innocenzi, A., Perani, L., Antonini, S., Sambasivan, R., Brunelli, S., Tajbakhsh, S. *et al.* (2011) Pericytes resident in postnatal skeletal muscle differentiate into muscle fibres and generate satellite cells. *Nat. Commun.*, **2**, 499.
 44. Sampaolesi, M., Torrente, Y., Innocenzi, A., Tonlorenzi, R., D'Antona, G., Pellegrino, M.A., Barresi, R., Bresolin, N., De Angelis, M.G.C., Campbell, K.P. *et al.* (2003) Cell therapy of alpha-sarcoglycan null dystrophic mice through intra-arterial delivery of mesoangioblasts. *Science*, **301**, 487–492.
 45. Sampaolesi, M., Blot, S., D'Antona, G., Granger, N., Tonlorenzi, R., Innocenzi, A., Mogno, P., Thibaud, J.-L., Galvez, B.G., Barthélémy, I. *et al.* (2006) Mesoangioblast stem cells ameliorate muscle function in dystrophic dogs. *Nature*, **444**, 574–579.
 46. Palumbo, R., Sampaolesi, M., De Marchis, F., Tonlorenzi, R., Colombetti, S., Mondino, A., Cossu, G. and Bianchi, M.E. (2004) Extracellular HMGB1, a signal of tissue damage, induces mesoangioblast migration and proliferation. *J. Cell Biol.*, **164**, 441–449.
 47. Tedesco, F.S., Hoshiya, H., D'Antona, G., Gerli, M.F.M., Messina, G., Antonini, S., Tonlorenzi, R., Benedetti, S., Berghella, L., Torrente, Y. *et al.* (2011) Stem cell-mediated transfer of a human artificial chromosome ameliorates muscular dystrophy. *Sci. Transl. Med.*, **3**, 96ra78.
 48. Domi, T., Porrello, E., Velardo, D., Capotondo, A., Biffi, A., Tonlorenzi, R., Amadio, S., Ambrosi, A., Miyagoe-Suzuki, Y., Takeda, S. *et al.* (2015) Mesoangioblast delivery of miniagrin ameliorates murine model of merosin-deficient congenital muscular dystrophy type 1A. *Skeletal Muscle*, **5**, 30.
 49. Cossu, G., Previtali, S.C., Napolitano, S., Cicalese, M.P., Tedesco, F.S., Nicastro, F., Novello, M., Roostalu, U., Natali, Sora, M.G., Scarlato, M. *et al.* (2015) Intra-arterial transplantation of HLA-matched donor mesoangioblasts in Duchenne muscular dystrophy. *EMBO Mol. Med.*, e201505636.
 50. Schrepfer, S., Deuse, T., Reichenspurner, H., Fischbein, M.P., Robbins, R.C. and Pelletier, M.P. (2007) Stem cell transplantation: the lung barrier. *Transplant. Proc.*, **39**, 573–576.
 51. Sharma, R.R., Pollock, K., Hubel, A. and McKenna, D. (2014) Mesenchymal stem or stromal cells: a review of clinical applications and manufacturing practices. *Transfusion*, **54**, 1418–1437.
 52. Yaffe, D. and Saxel, O. (1977) Serial passaging and differentiation of myogenic cells isolated from dystrophic mouse muscle. *Nature*, **270**, 725–727.
 53. Tonlorenzi, R., Dellavalle, A., Schnapp, E., Cossu, G. and Sampaolesi, M. (2007) Isolation and characterization of mesoangioblasts from mouse, dog, and human tissues. *Curr. Protoc. Stem Cell Biol.*, doi:10.1002/9780470151808.sc02b01s3.
 54. Di Matteo, M., Samara-Kuko, E., Ward, N.J., Waddington, S.N., McVey, J.H., Chuah, M.K.L. and VandenDriessche, T. (2014) Hyperactive piggyBac transposons for sustained and robust liver-targeted gene therapy. *Mol. Ther.*, **22**, 1614–1624.
 55. Li, X., Lobo, N., Bauser, C.A. and Fraser, M.J. (2001) The minimum internal and external sequence requirements for transposition of the eukaryotic transformation vector piggyBac. *Mol. Genet. Genomics*, **266**, 190–198.
 56. Li, X., Harrell, R.A., Handler, A.M., Beam, T., Hennessy, K. and Fraser, M.J. (2005) piggyBac internal sequences are necessary for efficient transformation of target genomes. *Insect Mol. Biol.*, **14**, 17–30.
 57. Li, X., Eastman, E.M., Schwartz, R.J. and Draghia-Akli, R. (1999) Synthetic muscle promoters: activities exceeding naturally occurring regulatory sequences. *Nat. Biotechnol.*, **17**, 241–245.
 58. Koo, T., Malerba, A., Athanasopoulos, T., Trollet, C., Boldrin, L., Ferry, A., Popplewell, L., Foster, H., Foster, K. and Dickson, G. (2011) Delivery of AAV2/9-microdystrophin genes incorporating helix 1 of the coiled-coil motif in the C-terminal domain of dystrophin improves muscle pathology and restores the level of α 1-syntrophin and α -dystrobrevin in skeletal muscles of mdx mice. *Hum. Gene Ther.*, **22**, 1379–1388.
 59. Athanasopoulos, T., Foster, H., Foster, K. and Dickson, G. (2011) Codon optimization of the microdystrophin gene for Duchenne muscular dystrophy gene therapy. *Methods Mol. Biol.*, **709**, 21–37.
 60. VandenDriessche, T., Ivics, Z., Izsvák, Z. and Chuah, M.K.L. (2009) Emerging potential of transposons for gene therapy and generation of induced pluripotent stem cells. *Blood*, **114**, 1461–1468.
 61. Kimura, E., Han, J.J., Li, S., Fall, B., Ra, J., Haraguchi, M., Tapscott, S.J. and Chamberlain, J.S. (2008) Cell-lineage regulated myogenesis for dystrophin replacement: a novel therapeutic approach for treatment of muscular dystrophy. *Hum. Mol. Genet.*, **17**, 2507–2517.
 62. Ross, J.J., Hong, Z., Willenbring, B., Zeng, L., Isenberg, B., Lee, E.H., Reyes, M., Keirstead, S.A., Weir, E.K., Tranquillo, R.T. *et al.* (2006) Cytokine-induced differentiation of multipotent adult progenitor cells into functional smooth muscle cells. *J. Clin. Invest.*, **116**, 3139–3149.
 63. Livak, K.J. and Schmittgen, T.D. (2001) Analysis of relative gene expression data using real-time quantitative PCR and the $2^{-\Delta\Delta C(T)}$ Method. *Methods*, **25**, 402–408.
 64. Rincon, M.Y., Sarcar, S., Danso-Abeam, D., Keyaerts, M., Matrai, J., Samara-Kuko, E., Acosta-Sanchez, A., Athanasopoulos, T., Dickson, G., Lahoutte, T. *et al.* (2014) Genome-wide computational analysis reveals cardiomyocyte-specific transcriptional cis-regulatory motifs that enable efficient cardiac gene therapy. *Mol. Ther.*, **23**, 43–52.
 65. Burnight, E.R., Staber, J.M., Korsakov, P., Li, X., Brett, B.T., Scheetz, T.E., Craig, N.L. and McCray, P.B. (2012) A hyperactive transposase promotes persistent gene transfer of a piggyBac DNA transposon. *Mol. Ther. Nucleic Acids*, **1**, e50.
 66. Sharma, N., Cai, Y., Bak, R.O., Jakobsen, M.R., Schröder, L.D. and Mikkelsen, J.G. (2013) Efficient sleeping beauty DNA transposition from DNA minicircles. *Mol. Ther. Nucleic Acids*, **2**, e74.
 67. Muses, S., Morgan, J.E. and Wells, D.J. (2011) A new extensively characterised conditionally immortal muscle cell-line for investigating therapeutic strategies in muscular dystrophies. *PLoS One*, **6**, e24826.
 68. Quattrocchi, M., Palazzolo, G., Floris, G., Schöffski, P., Anastasia, L., Orlicchio, A., Vandendriessche, T., Chuah, M.K.L., Cossu, G., Verfaillie, C. *et al.* (2011) Intrinsic cell memory reinforces myogenic commitment of pericyte-derived iPSCs. *J. Pathol.*, **223**, 593–603.
 69. Ley, D., Van Zwieten, R., Puttini, S., Iyer, P., Cochard, A. and Mermod, N. (2014) A PiggyBac-mediated approach for muscle gene transfer or cell therapy. *Stem Cell Res.*, **13**, 390–403.
 70. Muses, S., Morgan, J.E. and Wells, D.J. (2011) Restoration of dystrophin expression using the Sleeping Beauty transposon. *PLoS Curr.*, **3**, RRN1296.
 71. Filareto, A., Parker, S., Darabi, R., Borges, L., Iacovino, M., SchAAF, T., Mayerhofer, T., Chamberlain, J.S., Ervasti, J.M., McIvor, R.S. *et al.* (2013) An ex vivo gene therapy approach to treat muscular dystrophy using inducible pluripotent stem cells. *Nat. Commun.*, **4**, 1549.
 72. Nakazawa, Y., Huye, L.E., Dotti, G., Foster, A.E., Vera, J.F., Manuri, P.R., June, C.H., Rooney, C.M. and Wilson, M.H. (2009) Optimization of the PiggyBac transposon system for the sustained genetic modification of human T lymphocytes. *J. Immunother.*, **32**, 826–836.
 73. Belay, E., Dastidar, S., VandenDriessche, T. and Chuah, M.K.L. (2011) Transposon-mediated gene transfer into adult and induced pluripotent stem cells. *Curr. Gene Ther.*, **11**, 406–413.
 74. Kouprina, N., Tomilin, A.N., Masumoto, H., Earnshaw, W.C. and Larionov, V. (2014) Human artificial chromosome-based gene delivery vectors for biomedicine and biotechnology. *Expert Opin. Drug Deliv.*, **11**, 517–535.
 75. Tedesco, F.S. (2015) Human artificial chromosomes for Duchenne muscular dystrophy and beyond: challenges and hopes. *Chromosome Res.*, **23**, 135–141.
 76. Hoshiya, H., Kazuki, Y., Abe, S., Takiguchi, M., Kajitani, N., Watanabe, Y., Yoshino, T., Shirayoshi, Y., Higaki, K., Messina, G. *et al.* (2009) A highly stable and nonintegrated human artificial chromosome (HAC) containing the 2.4 Mb entire human dystrophin gene. *Mol. Ther.*, **17**, 309–317.

77. Kazuki, Y., Hiratsuka, M., Takiguchi, M., Osaki, M., Kajitani, N., Hoshiya, H., Hiramatsu, K., Yoshino, T., Kazuki, K., Ishihara, C. *et al.* (2010) Complete genetic correction of ipsc cells from Duchenne muscular dystrophy. *Mol. Ther.*, **18**, 386–393.
78. Tedesco, F.S., Gerli, M.F.M., Perani, L., Benedetti, S., Ungaro, F., Cassano, M., Antonini, S., Tagliafico, E., Artusi, V., Longa, E. *et al.* (2012) Transplantation of genetically corrected human iPSC-derived progenitors in mice with limb-girdle muscular dystrophy. *Sci. Transl. Med.*, **4**, 140ra89.
79. Arechavala-Gomez, V., Anthony, K., Morgan, J. and Muntoni, F. (2012) Antisense oligonucleotide-mediated exon skipping for Duchenne muscular dystrophy: progress and challenges. *Curr. Gene Ther.*, **12**, 152–160.
80. Echigoya, Y. and Yokota, T. (2014) Skipping multiple exons of dystrophin transcripts using cocktail antisense oligonucleotides. *Nucleic Acid Ther.*, **24**, 57–68.
81. Li, H.L., Fujimoto, N., Sasakawa, N., Shirai, S., Ohkame, T., Sakuma, T., Tanaka, M., Amano, N., Watanabe, A., Sakurai, H. *et al.* (2015) Precise correction of the dystrophin gene in duchenne muscular dystrophy patient induced pluripotent stem cells by TALEN and CRISPR-Cas9. *Stem Cell Rep.*, **4**, 143–154.
82. Ousterout, D.G., Kabadi, A.M., Thakore, P.I., Perez-Pinera, P., Brown, M.T., Majoros, W.H., Reddy, T.E. and Gersbach, C.A. (2015) Correction of dystrophin expression in cells from duchenne muscular dystrophy patients through genomic excision of exon 51 by zinc finger nucleases. *Mol. Ther.*, **23**, 523–532.
83. Ousterout, D.G., Kabadi, A.M., Thakore, P.I., Majoros, W.H., Reddy, T.E. and Gersbach, C.A. (2015) Multiplex CRISPR/Cas9-based genome editing for correction of dystrophin mutations that cause Duchenne muscular dystrophy. *Nat. Commun.*, **6**, 6244.
84. Mátés, L., Chuah, M.K.L., Belay, E., Jerchow, B., Manoj, N., Acosta-Sanchez, A., Grzela, D.P., Schmitt, A., Becker, K., Matrai, J. *et al.* (2009) Molecular evolution of a novel hyperactive Sleeping Beauty transposase enables robust stable gene transfer in vertebrates. *Nat. Genet.*, **41**, 753–761.
85. Belay, E., Matrai, J., Acosta-Sanchez, A., Ma, L., Quattrocchi, M., Mátés, L., Sancho-Bru, P., Geraerts, M., Yan, B., Vermeesch, J. *et al.* (2010) Novel hyperactive transposons for genetic modification of induced pluripotent and adult stem cells: a nonviral paradigm for coaxed differentiation. *Stem Cells*, **28**, 1760–1771.
86. Grabundzija, I., Irgang, M., Mátés, L., Belay, E., Matrai, J., Gogol-Döring, A., Kawakami, K., Chen, W., Ruiz, P., Chuah, M.K.L. *et al.* (2010) Comparative analysis of transposable element vector systems in human cells. *Mol. Ther.*, **18**, 1200–1209.
87. Krieg, A.M., Yi, A.K., Matson, S., Waldschmidt, T.J., Bishop, G.A., Teasdale, R., Koretzky, G.A. and Klinman, D.M. (1995) CpG motifs in bacterial DNA trigger direct B-cell activation. *Nature*, **374**, 546–549.
88. Reyes-Sandoval, A. and Ertl, H.C.J. (2004) CpG methylation of a plasmid vector results in extended transgene product expression by circumventing induction of immune responses. *Mol. Ther.*, **9**, 249–261.
89. Yew, N.S., Przybylska, M., Ziegler, R.J., Liu, D. and Cheng, S.H. (2001) High and sustained transgene expression in vivo from plasmid vectors containing a hybrid ubiquitin promoter. *Mol. Ther.*, **4**, 75–82.
90. Hyde, S.C., Pringle, I.A., Abdullah, S., Lawton, A.E., Davies, L.A., Varathalingam, A., Nunez-Alonso, G., Green, A.-M., Bazzani, R.P., Sumner-Jones, S.G. *et al.* (2008) CpG-free plasmids confer reduced inflammation and sustained pulmonary gene expression. *Nat. Biotechnol.*, **26**, 549–551.
91. Lukacs, G.L., Haggie, P., Seksek, O., Lechardeur, D., Freedman, N. and Verkman, A.S. (2000) Size-dependent DNA mobility in cytoplasm and nucleus. *J. Biol. Chem.*, **275**, 1625–1629.
92. Cadiñanos, J. and Bradley, A. (2007) Generation of an inducible and optimized piggyBac transposon system. *Nucleic Acids Res.*, **35**, e87.
93. Biasco, L., Baricordi, C. and Aiuti, A. (2012) Retroviral integrations in gene therapy trials. *Mol. Ther.*, **20**, 709–716.
94. Wilson, M.H. and George, A.L. (2010) Designing and testing chimeric zinc finger transposases. *Methods Mol. Biol.*, **649**, 353–363.
95. Kettlun, C., Galvan, D.L., George, A.L., Kaja, A. and Wilson, M.H. (2011) Manipulating piggyBac transposon chromosomal integration site selection in human cells. *Mol. Ther.*, **19**, 1636–1644.
96. Wells, D.J., Wells, K.E., Asante, E.A., Turner, G., Sunada, Y., Campbell, K.P., Walsh, F.S. and Dickson, G. (1995) Expression of human full-length and minidystrophin in transgenic mdx mice: implications for gene therapy of Duchenne muscular dystrophy. *Hum. Mol. Genet.*, **4**, 1245–1250.
97. Neri, M., Torelli, S., Brown, S., Ugo, I., Sabatelli, P., Merlini, L., Spitali, P., Rimessi, P., Gualandi, F., Sewry, C. *et al.* (2007) Dystrophin levels as low as 30% are sufficient to avoid muscular dystrophy in the human. *Neuromuscul. Disord.*, **17**, 913–918.
98. Holliday, R. (2014) The commitment of human cells to senescence. *Interdiscip. Top. Gerontol.*, **39**, 1–7.
99. Marg, A., Escobar, H., Gloy, S., Kufeld, M., Zacher, J., Spuler, A., Birchmeier, C., Izsvák, Z. and Spuler, S. (2014) Human satellite cells have regenerative capacity and are genetically manipulable. *J. Clin. Invest.*, **124**, 4257–4265.
100. Costamagna, D., Berardi, E., Ceccarelli, G. and Sampaolesi, M. (2015) Adult stem cells and skeletal muscle regeneration. *Curr. Gene Ther.* **15**, 348–363.
101. Gerli, M.F.M., Maffioletti, S.M., Millet, Q. and Tedesco, F.S. (2014) Transplantation of induced pluripotent stem cell-derived mesoangioblast-like myogenic progenitors in mouse models of muscle regeneration. *J. Vis. Exp.*, **83**, e50532.
102. Maffioletti, S.M., Gerli, M.F.M., Ragazzi, M., Dastidar, S., Benedetti, S., Loperfido, M., VandenDriessche, T., Chuah, M.K. and Tedesco, F.S. (2015) Efficient derivation and inducible differentiation of expandable skeletal myogenic cells from human ES and patient-specific iPSC cells. *Nat. Protoc.*, **10**, 941–958.
103. Loperfido, M., Steele-Stallard, H.B., Tedesco, F.S. and VandenDriessche, T. (2015) Pluripotent Stem Cells for Gene Therapy of Degenerative Muscle Diseases. *Curr. Gene Ther.* **15**, 364–380.